Novel Biomechanical and Biochemical Signatures of Post-Traumatic Osteoarthritis: A Murine Model Study

A Thesis

Submitted to the Faculty

of

Drexel University

by

Emilia Marie Roberts

in partial fulfillment of the

requirements for the degree

of

Masters of Science in Biomedical Engineering

June 2016

Acknowledgements

I would like to express my sincere gratitude to Drexel University, and the School of Biomedical Engineering and Sciences for allowing me to continue my passion at the graduate level. I want to thank and acknowledge my thesis advisor Dr. Lin Han for allowing me to join his laboratory and for his guidance and expertise in developing my project. I also want to thank all my lab-mates in Han Laboratory, not only for training and collaboration, but for the sense of camaraderie we developed when working together. I am grateful for the planning and help of Carolyn Riley, my academic advisor for my time at Drexel University. Finally, to all my friends and family who encouraged me to pursue a thesis project, and pushed me to do my very best.

Table of Contents

List of Tables

List of Figures

Abstract

Investigations into the Biomechanical and
Biochemical Outcomes of Post-Traumatic Osteoarthritis
Emilia M. Roberts
Lin Han, Ph.D.

Post-traumatic osteoarthritis (PTOA) is an inflammatory-based cartilage degenerating disease that develops after joint injury. It results in the breakdown of articular cartilage in the joints, leading to pain and loss of mobility over time, eventually requiring surgical intervention. Approximately 50% of patients who suffer a serious joint injury such as an anterior cruciate ligament (ACL) tear will develop diagnosable PTOA within 10-15 years. In the United States, more than 5 million people have various degrees of PTOA in the hip, ankle, or knee. Despite its prevalence, there are few treatments for cartilage injury, with most medical intervention centered around palliative care once PTOA has been diagnosed. Pharmacological solutions are limited, due to the complexity and difficulty of studying chondrocyte behavior and the cartilage matrix structure-function relationship in vivo.

In this study, cartilage injury was induced in a murine model by the destabilization of the medial meniscus (DMM) surgery on the right knee joint. After the procedure, chondrocyte signaling behavior was studied by examining the expression of bone morphogenetic protein-2 (BMP2) and its associated intracellular downstream mediator, pSmad1/5/8, using immunohistochemistry. These two proteins are important homeostatic cytokines in cartilage, instructing chondrocytes to synthesize new extra-cellular matrix (ECM), mainly type II collagen and aggrecan. Changes in the matrix

structure of cartilage were examined via changes in aggrecan and decorin. Aggrecan is a large, highly charged protein that binds to water, reducing its flow, and giving cartilage its innate force-cushioning properties. Decorin is an important, small leucine-rich proteoglycan, which regulates the formation and homeostasis of cartilage ECM through binding to other proteoglycans, such as aggrecan. In addition, changes in function-relevant mechanical properties were also examined by atomic force microscopy (AFM)-based Nanoindentation on condyle cartilage surfaces.

After the DMM surgery, cartilage homeostasis was disrupted. BMP2 and pSmad1/5/8 staining increased, suggesting anabolic and catabolic changes to chondrocyte function. Aggrecan concentration was reduced, signifying degradation of the ECM. Meanwhile, the active involvement of decorin in the ECM degradation process is indicated by the substantial reduction of aggrecan in decorin-null mice. Furthermore, cartilage after DMM showed significantly lower nanoindentation modulus than the control after Sham surgery, highlighting OA-induced loss of joint function. These biochemical and biomechanical results prove insights into the concomitant biological and biomechanical changes of cartilage during the progression of injury-induced PTOA.

Chapter 1: Introduction and Specific Aims

1.1: Post Traumatic Osteoarthritis

Post-traumatic osteoarthritis, otherwise known as PTOA, is a degenerative disease where inflammation caused by injury to the joint results in the damaging and wearing down of joint cartilage. PTOA most commonly occurs in people who have experienced a traumatic joint injury, such as a torn ligament or meniscus [1]. Although the majority of osteoarthritis cases (OA) arise from more natural wearing down of cartilage, primarily in old age, a substantial amount of cases of OA (12%) occur due to injury [1]. The secondary-to-injury form of OA typically progresses more quickly than primary OA [2], resulting in worse patient outcomes in a smaller amount of time.

PTOA can develop in any joint that suffers injury, most commonly in the knee, hip, and ankle joints. There are a wide range of injuries that can lead to the development of post traumatic osteoarthritis, including sports injuries, vehicle accidents, and simple falls. Any type of trauma to a joint can lead to osteoarthritis down the road, although load-bearing joints such as the knee or ankle are at greater risk. Joint injuries including direct and indirect joint impact loading, meniscal, ligament and joint capsule tears, joint dislocations and intra-articular fractures, increase the risk of progressive joint degeneration that causes posttraumatic OA [3].

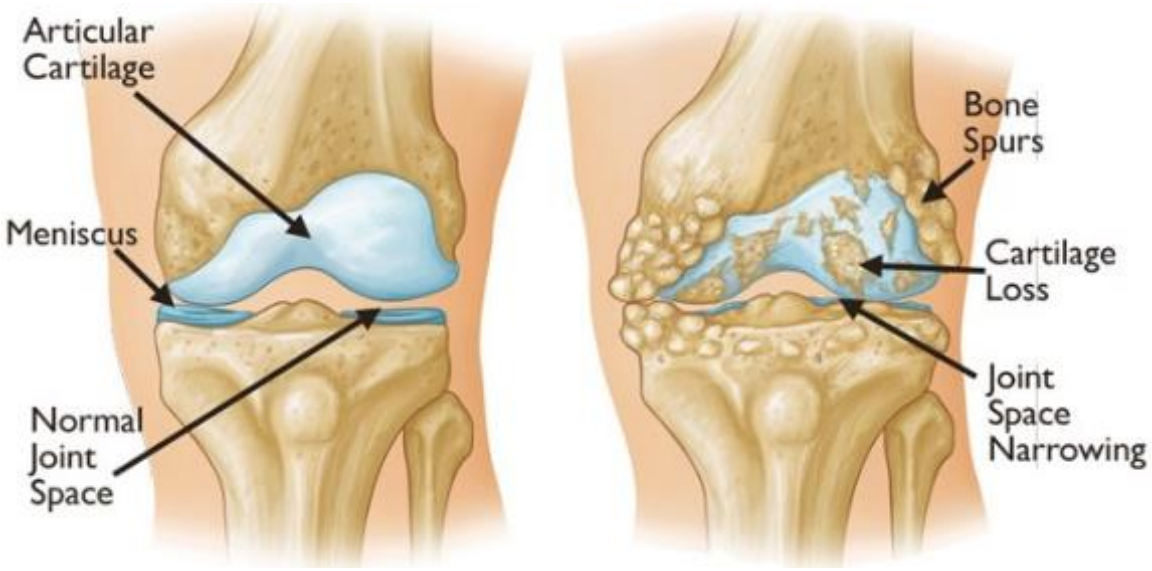

Figure 1: Comparison of healthy and osteoarthritic joint. Note structural changes, most specifically the narrowing of the joint space, which is commonly used to diagnose OA radiographically (adapted from AAOS.org).

Despite post-traumatic osteoarthritis's life-changing effects, there are few studies on the total number of patients affected by PTOA. A research group from the University of Iowa Hospitals and Clinics estimates that 5.6 million individuals in the United States alone have some form of knee, hip, or ankle PTOA [4]. The same group also estimates that PTOA causes approximately 3 billion dollars of financial burden annually in the Unites States [4].

PTOA is especially severe in younger patient populations, as a patient who develops PTOA at 18 years old due to an injury will most likely have severe pain and will have to go through several knee surgeries over the course of their life. A large portion of these injuries can be attributed to injuries to the anterior cruciate ligament (ACL). About 50% of patients who injure their ACL will develop PTOA within 10-15 years of the injury [2], even considering the treatment options available today. Women are even more at risk than men are following an ACL injury, with 51% of women (mean

age 31 years) had radiographic diagnosed OA [5] compared to 41% of men (mean age 38 years) [6]post injury. Both women and men in these studies reported knee pain and functional limitations resulting in lifestyle modifications for 50% of the women and for 30% of the men [5],[6]. Another study conducted in Sweden found that patients who receive cruciate ligament reconstructive surgery did not show a protective effect on knee OA in the long term [7]. Considering that the subjects of these studies were younger individuals injured during sports activities, lifestyle changes would have to occur for the rest of the patient's life (>30 years).

1.2: Predictors and Outcomes of Post-Traumatic Osteoarthritis

The pathogenesis of PTOA is not fully understood. The complicated network of pathways and outcomes makes post-traumatic osteoarthritis difficult to treat either surgically or pharmaceutically. Research is needed to better clarify how these factors contribute to the development of PTOA and to develop tailored treatment programs that consist of both acute biologic interventions targeted to decrease inflammation and cellular death in response to injury and improved surgical methods to restore stability, congruity, and alignment [8].

The development of PTOA (at the cartilage level) following an injury is broken down into three stages; immediate (within seconds), acute (within months), and chronic (within years) [9]. The following table lists some of the outcomes.

Table 1: Pathogenesis of PTOA damage on different time scales (adapted from Lotz et al [9]).

Immediate (seconds)	Acute (months)	Chronic (years)
Cell necrosis	Apoptosis	Joint tissue remodeling
Collagen rupture	Leukocyte infiltration	
Glycosaminoglycan loss	Inflammatory Mediators	
Hemarthrosis	Extracellular matrix degradation	Inflammation
	Deficient lubricants	
	Arthrofibrosis	

The immediate effects of joint injury are often evident, as mechanical overload can cause bone fracture, ruptured ligaments, tendons and menisci, and compressive and shear damage to cartilage. The mechanical damage needs to be repaired surgically, increasing patient risks of adverse outcomes. Despite advances in orthopedic surgical techniques, many patients will develop degenerative PTOA following a traumatic joint injury.

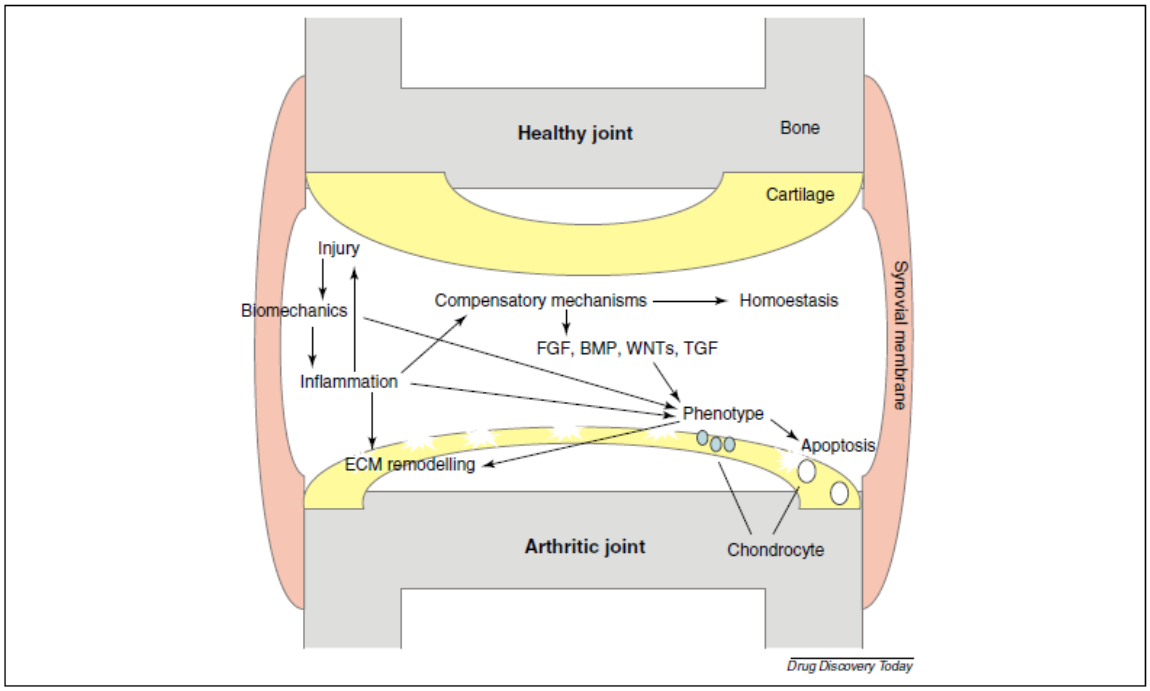

Figure 2: Graphic showing different pathways of cartilage degradation following a traumatic injury, chief among which is inflammation. Adapted from Sherwood et al [10].

The immediate cellular-level factor of PTOA after cartilage injury is that of cell death, specifically chondrocyte death [11]. Cell death after injury happens in two "waves", the immediate cell death via necrosis that occurs immediately after injury, and cell death that is induced via secreted apoptosis factors. The secondary cells may not be affected by the impact injury at all, but will be induced to die via cell necrosis factors and inflammatory effects [11]. Some chondrocytes have the ability to survive the cytokine induced death response via autophagy (rapidly processing abnormal cytosolic proteins/organelles), the ability is reduced in OA cartilage [12].

Another immediate factor that might be overlooked is intra-articular bleeding into the synovial fluid of the damaged joint. Bleeding might be overlooked in the face of severe mechanical damage, but it is common after injury and is another factor that must be examined to fully understand the development of PTOA. Intra-articular bleeding is observed in 90% of severe (requiring surgical intervention) joint injuries [13]. Hemarthrosis leads to via induced chondrocyte apoptosis and glycosaminoglycan (GAG) loss [13] while blocking the synthesis of new proteoglycans, indicating that hemarthrosis effects both anabolic and catabolic chondrocyte processes.

Moving into the acute (months) effects of cartilage injury, chronic inflammation of the synovial capsule and cartilage itself must be considered. Interleukin-1 (IL-1) and other inflammatory cytokines in its family are overexpressed after mechanical joint injury, and increases in expression are correlated with severity of cartilage damage [14]. Over time, the cartilage will begin to breakdown as the catabolic and anabolic processes that regulate cartilage structure and function begin to result in cartilage degradation. There is conflicting evidence pointing at a complicated cytokine homeostasis in cartilage,

both in healthy and osteoarthritic tissue. Immediately after injury, inflammatory cytokines such as IL-1 and TNF-alpha are upregulated. However, established arthritic tissue has lower levels of inflammatory cytokines than healthy tissue [15], indicating that brief spikes of cytokine upregulation can have damaging effects in the longer term.

Two more important cellular signaling pathways in cartilage are the BMP and TGF-β pathways. Both pathways increase proteoglycan synthesis when injected. TGF-β, when injected, resulted in OA-like lesions, while inhibiting it completely lead to cartilage destruction [16]. Completely blocking BMP signaling had a similar result [16]. The conflicting conclusions of these studies emphasize the complex balance of signaling cytokines in both healthy and damaged cartilage.

1.3: PTOA Diagnosis and Treatment

PTOA is usually diagnosed after the patient is starting to notice symptoms such as pain and reduction of joint mobility. The treating doctor will examine patient medical history, such as injuries to the offending joint. To confirm, imaging techniques such as x-ray, CT, or MRI imaging is used to give an official diagnosis of osteoarthritis using an established grading protocol, the Kellgren and Lawrence Classification (KL grade) [17]. In brief, a grade 0 shows no radiographic features of OA, while the most severe, grade 4, large osteophytes, severe joint space narrowing and sclerosis, and the presence of bony deformities.

After diagnosis, there are two stages to treating PTOA. The first is palliative treatment, to try and make the joint more comfortable for the patient and to slow down

the increase of severity of the condition. Knee injury prevention, rehabilitation after knee injuries, regular exercise, maintaining body weight, and a changed locomotion pattern may prevent osteoarthritis initiation and progression in young adults [18]. Certain chemical treatments are also used, such as steroidal injections to reduce inflammation, and artificial synovial fluid injections to help increase joint space and reduce pain. Palliative treatments can help to slow the progression of osteoarthritis, although many patients will require the second step of treatment, a surgical solution, such as a knee or hip partial or total replacement.

Unfortunately, the surgical solution is not always an effective treatment for younger patients, considering the average lifespan of medical devices designed to treat PTOA (~20 years on average) [19]. Young patients will need to have multiple devices implanted through their lifetime, increasing risks for surgical complications and other issues. Research into improving patient outcomes is occurring from two directions; from the patient end (slowing the development from mild OA to severe), and the device end (improving medical implant function and durability).

Pharmacological treatment of post-traumatic osteoarthritis will have to take into account the complex web of different cytokines, regional structural differences, and different healthy homeostatic baselines from patient to patient [20]. The disruption of cartilage homeostasis by arthritic mechanisms is a primary target for treatments. Maintaining normal homeostasis in mechanically damaged cartilage could not only help to prevent the development of POTA, but also to help maintain healthy cartilage as patient's age. Considering the complexity of cartilage homeostasis, there are many different pharmacological targets that could be used individually or in compound

treatments to prevent or treat PTOA. An individualized pharmacological solution based on the patient's baseline cartilage homeostasis would be the most effective option.

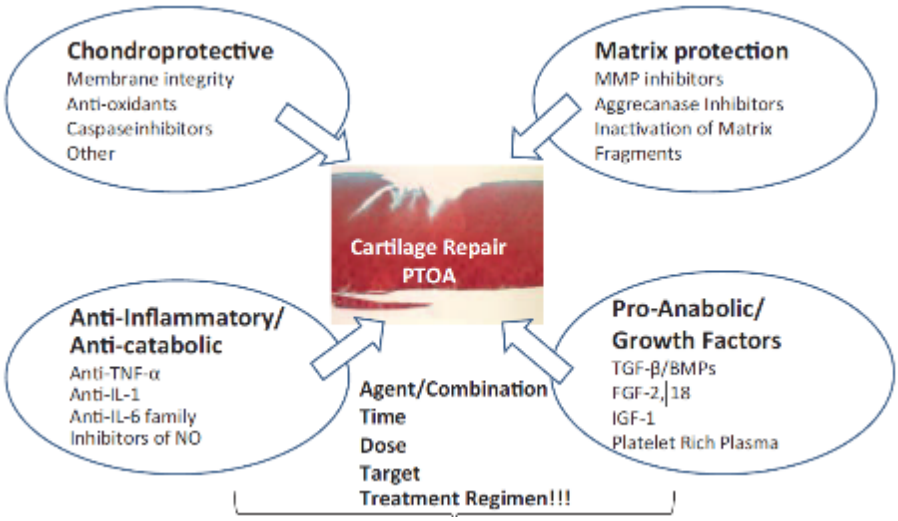

Figure 3: Figure showing different aspects to consider for treatment of cartilage damage following mechanical injury. It is most important to protect chondrocytes, in addition to helping maintain their normal function [20].

1.4: Murine Models of Post-Traumatic Osteoarthritis

There have been many in-vitro human studies of osteoarthritis, bringing insight to the cellular responses and molecular pathways of PTOA. That being said, they still cannot replicate the complicated network of tissue interactions, biological stimuli, and long time-scale in an in-vivo model [21]. Additionally, human tissue past the cellular level is expensive and can be hard to work with. More and more research groups are moving towards using mice as a substitute. Experiments using murine samples are cheaper, faster, and more flexible, allowing for controlled different genotypes (genetic knockout mice) and longer time-scales (can study months after injury). Studying how

different genotypes of mice respond to an induced cartilage injury model leads to major discoveries about how different cellular pathways influence chondrocyte behavior.

In order to study cartilage degradation after injury in-vivo, a murine model of injury must be developed. There are several different ways to induce an injury in a murine model, with the two major kinds being chemically induced injury, and mechanically induced injury. A single-incident, mechanically induced injury most closely simulates PTOA in humans, as often a single serious joint injury leads to the development of cartilage degradation in humans. An example is the DMM procedure, where a surgeon cuts the medial meniscus tendon, destabilizing the medial meniscus of the knee joint. The DMM procedure results in OA-like symptoms quickly and in reproducible fashion in mice [22]. The DMM procedure and its outcomes will be discussed in more detail in the methods section of this thesis.

One of the most common methods of examining the severity of osteoarthritis is being using histology. Histology is the method of staining thin sections of the joint space, allowing researchers and pathologists to examine the cartilage surface for changes compared to normal tissue. There are many different stains, but the most common type for studying cartilage is safranin-O/Fast Green (stains cartilage red with a green background). Safranin-O/Fast Green staining is useful for classifying the severity of cartilage damage, using a scoring system that takes types and prevalence of damage into account. There are many different scoring systems, but most take into account cartilage surface damage, lesion formation, synovial and bone alterations, and cartilage thickness [23]. Histological examinations only give information on a macro scale about the structural integrity of the cartilage, with little insight into the behavior of the cells and

individual components of the cartilage matrix. The method of immunohistochemistry, using antibodies that bind and stain for specific components allows researchers to examine the complicated cellular pathways, in addition to individual structural components. There are other methods of looking at chondrocyte behavior, such as measuring DNA and RNA expression levels, but these involve isolating the chondrocytes from their cartilage matrix, potentially effecting measured levels.

Overall, animal models of PTOA, specifically mouse models, give researchers much more flexibility in examining the complicated interactions between tissues, cells, and other biological stimuli in osteoarthritis. That being said, some care must be taken that sufficient cross-translational research is conducted before brining any promising treatments from animal studies to the pre-clinical testing in humans.

1.5: Thesis Specific Aims

Aim 1: To investigate changes of a bio-chemical nature during the development of post-traumatic osteoarthritis in a murine model using immune-histological methods.

Aim 2: To investigate changes of a bio-mechanical nature during the development of post-traumatic osteoarthritis in a murine model. This is to be done using a Bruker Atomic Force Microscope (AFM), to evaluate mechanical changes during the development of PTOA murine model.

Chapter 2: Methods Background

2.1: Modeling PTOA: Destabilization of the Medial Meniscus

Mice can develop osteoarthritis in the later stages of their life, and there are documented cases of earlier-developing cartilage degradation following injury. However, a naturally occurring injury is not nearly consistent or repeatable enough to be considered for modeling human cartilage degradation following injury. Glasson et al [22] developed a surgery known as the destabilization of the medial meniscus (DMM) in order to induce injury-based cartilage degradation.

In the DMM surgery, the medial meniscotibial ligament is transected without damage to other tissues, allowing the medial meniscus free movement in the joint.

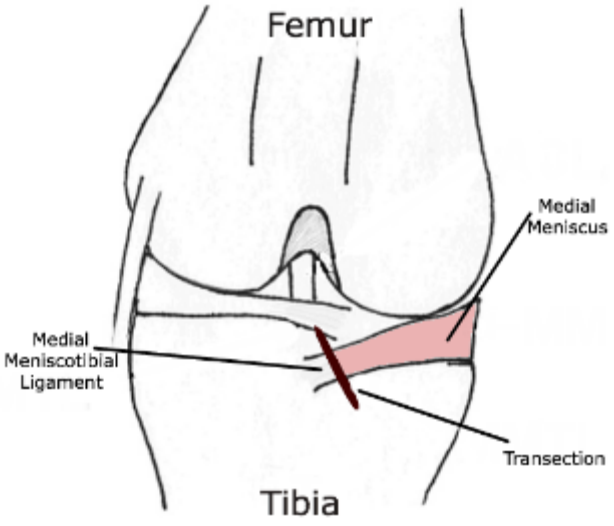

Figure 4: Dissection diagram for DMM showing transection cut of medial meniscus. The surgery causes minimal tissue damage to surrounding joint tissue while causing joint instability on the medial side. Adapted from Glasson et al [22].

Under Sham, the left joint capsule was opened in the same fashion to expose the ligament but without any further damage. The movement of the medial meniscus medially results in an increase in mechanical stress on the medial side of the joint.

After 4 and 8 weeks, mice are sacrificed and the DMM and Sham knee joints were examined and scored using histological methods, specifically Safranin-O/Fast green staining as mentioned in the introduction. At 4 weeks, DMM mice had knees classified as mild-to-moderate OA, while at 8 weeks they were classified as moderate OA, increasing in severity up to 12 weeks post-surgery [22]. The slower developing osteoarthritic symptoms more closely model that of post-traumatic osteoarthritis in humans. This distinction is important, since some other injury induced models, such as the anterior cruciate ligament transection model, quickly developing, severe OA in mice. The DMM procedure progresses that allows for the stages of OA development to be observed, and most importantly lesion severity and location was similar to that of spontaneous murine osteoarthritis. Notably, male mice undergoing the DMM surgery develop more severe osteoarthritis post-surgery than female mice [24]. Because of this finding, only male mice were used in the experiments used to create this thesis.

The focus of the DMM surgery has been to study the roles of various molecular signaling pathways in PTOA, such as the roles of ADAMTS5 (the major aggrecanase in mouse cartilage) [25]and EGFR (epidermal growth factor receptor) [26] signaling in OA.

Post-mortem, the DMM murine joints can be processed for many different experiments, such as Nanoindentation, sectioning for histology and immunohistochemistry, scanning or tunneling electron microscopy of the cartilage surface, and mechanical properties testing via AFM.

2.2: Atomic Force Microscopy and Nanoindentation

2.2.1: AFM History and Introduction

Atomic force microscopy makes use of an important physical property known as piezoelectricity. A material is considered “piezoelectric” if a mechanical change induces an electrical field, or vice-versa. In the case of this microscope, the electrical field induced by the system moves a tipped cantilever into the sample, resulting in the calibrated cantilever bending, deflecting the laser. Calibrating the mechanical properties of the cantilever and measuring how far the laser moved via a photodiode deduces mechanical properties such as modulus, force-deformation curves, and even frictional force.

The atomic force microscope (AFM) was originally invented by IBM scientists Binning et al in 1985. At first, the AFM operated in contact mode, moving along the surface scanning as it went. It was difficult to scan without damaging biological tissue. Once tapping mode was developed, it became much easier to perform research and many multitudes of biological tissue. Study of bone and cartilage related tissues benefited greatly, as the mechanical properties are of the utmost importance when investigating different degenerative conditions, and therapeutic pathways related to these issues.

Nano-indentation is a mechanical testing method where a tipped cantilever is held against a substrate surface by applying a set current to the piezo of the AFM. Generally the sample will be indented in fluid conditions, in order to better simulate physiological conditions. Buffered saline such as PBS is usually used. A spherical or pyramidal tip is

programed to indent into the sample (cell or tissue) at a constant piezo displacement rate, ranging from ~0.05 to 10 μm/s (approximately the indentation depth rate), up to a preset maximum indentation force or depth [27]. During the indentation process, cantilever bending-induced laser movement is recorded by a photodetector. Based on the calibrated tip geometry and cantilever stiffness, the indentation force versus depth curve can be extracted. Under AFM, different indentation rates can be applied and compared to study the time-dependent poroviscoelastic properties of soft tissues, such as cartilage.

2.2.2: Nanoindentation Mechanism and Modeling

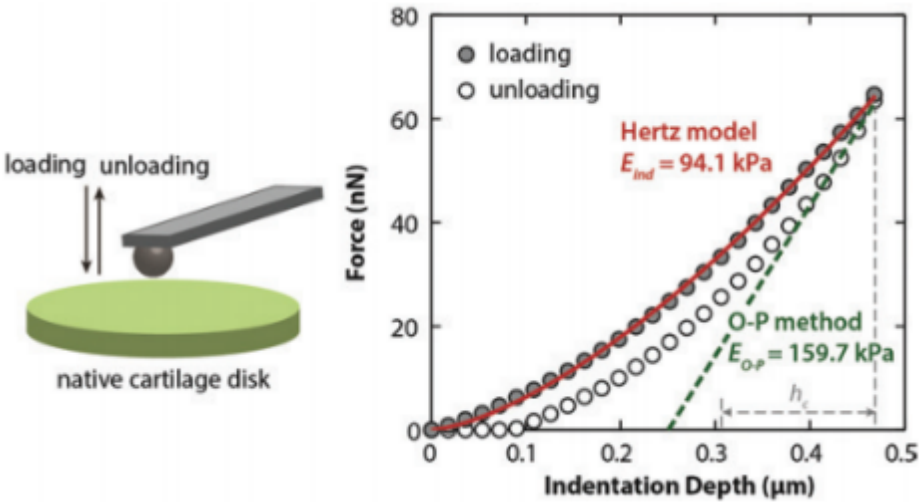

$$F = \frac{4}{3}\frac{E_{ind}}{(1-\nu^2)} R_r^{1/2} D^{3/2} \qquad \frac{1}{R_r} = \frac{1}{R_1} + \frac{1}{R_2}$$

Figure 5: Hertzian fitting of force-deformation curve to find indentation modulus (resistance to indentation). The graph shows fitting using the Hertzian model in red and Oliver-Pharr model (another model not used for this thesis) in green. Equation 1 is the Hertz Model. R_r as defined by equation 2 is the reduced contact radius, with R_1 being the indenter tip radius, and R_2 being curvature of the sample. For the rest of the variables of Eqn. 1, *v* is Poisson's ratio (around 0.1 for cartilage) of the sample, and D is the indentation depth. Figure adapted from Han et al [27].

From the force-deformation curves, the indentation modulus can be determined using the Hertz Model (Equation 1 of Figure 5), which takes into account the near-hyperbolic increase of tip-sample contact with indentation depth. The Hertz model can be used over the entire duration of the loading D-F curve as shown in Figure 5.Another approach (not used for data analysis in this thesis) is the Oliver–Pharr method that uses the initial slope of the unloading portion of force-deformation curves (top 25–75 %) to estimate the modulus. The O-P method was originally developed for testing on materials that only undergo elastic and plastic deformation (e.g. ceramics and metals).

There is a significant difference in calculated indentation modulus between the Hertz Model and the Oliver-Pharr Model (O-P model gives 1.7 times higher modulus). The values calculated from Hertz model from the loading curve represents an "effective indentation modulus" reflecting mostly the compressive resistance of cartilage at the given indentation rate. The unloading curve for cartilage likely includes the combined effects of both elastic recovery and poro-viscoelastic force relaxation, and thus, the elastic–plastic deformation assumption in the Oliver–Pharr method does not hold [27], resulting in the differences of calculated indentation moduli between the two models.

Although effective for determining relative indentation modulus, the Hertz model does not take into account the inherent viscoelasticity of cartilage, the mechanical nonlinearity [27]. For more comprehensive analysis of cartilage mechanical characteristics, more complicated, non-linear time-dependent mechanical models, such as the biphasic poroelastic model, are needed to accurately determine poroelastic and viscoelastic properties of cartilage.

NOTE: SEE APPENDIX FOR SPECIFIC AFM WORKING PROTOCOLS

2.3: Immunohistochemical Methods

Immunohistochemistry (IHC) is a specific subset of histology. At its most basic level, it uses the natural binding properties of antibodies to specific antigens (usually proteins) to create location specific markers to qualitatively detect presence and in some cases relative amounts of the target antigen. IHC was first developed by Dr. Albert Coons in 1941 [28], by using antibodies labeled with Fluorescein isothiocynate to determine local location of pneumococcal antigens in tissues. Since its introduction, several different labeling types have been used in conjunction with antibodies. These include fluorescent markers, enzyme-based markers, and in the past, even radioactive elements. IHC is a qualitative, rather than quantitative experimental technique (although some fluorescent stains can be used semi-quantitatively, since there is no endogenous or non-specific staining.)

In general, IHC is carried out in the following steps: First, a 4-10 μm thick tissue section is obtained, and mounted on slides, which are usually embedded in paraffin wax. De-paraffinize and rehydrate the tissue sections via a strong organic solvent such as xylene, and an alcohol gradient. An antigen retrieval step is often needed, due to the cross-linking of the fixing process (to stabilize the tissue).

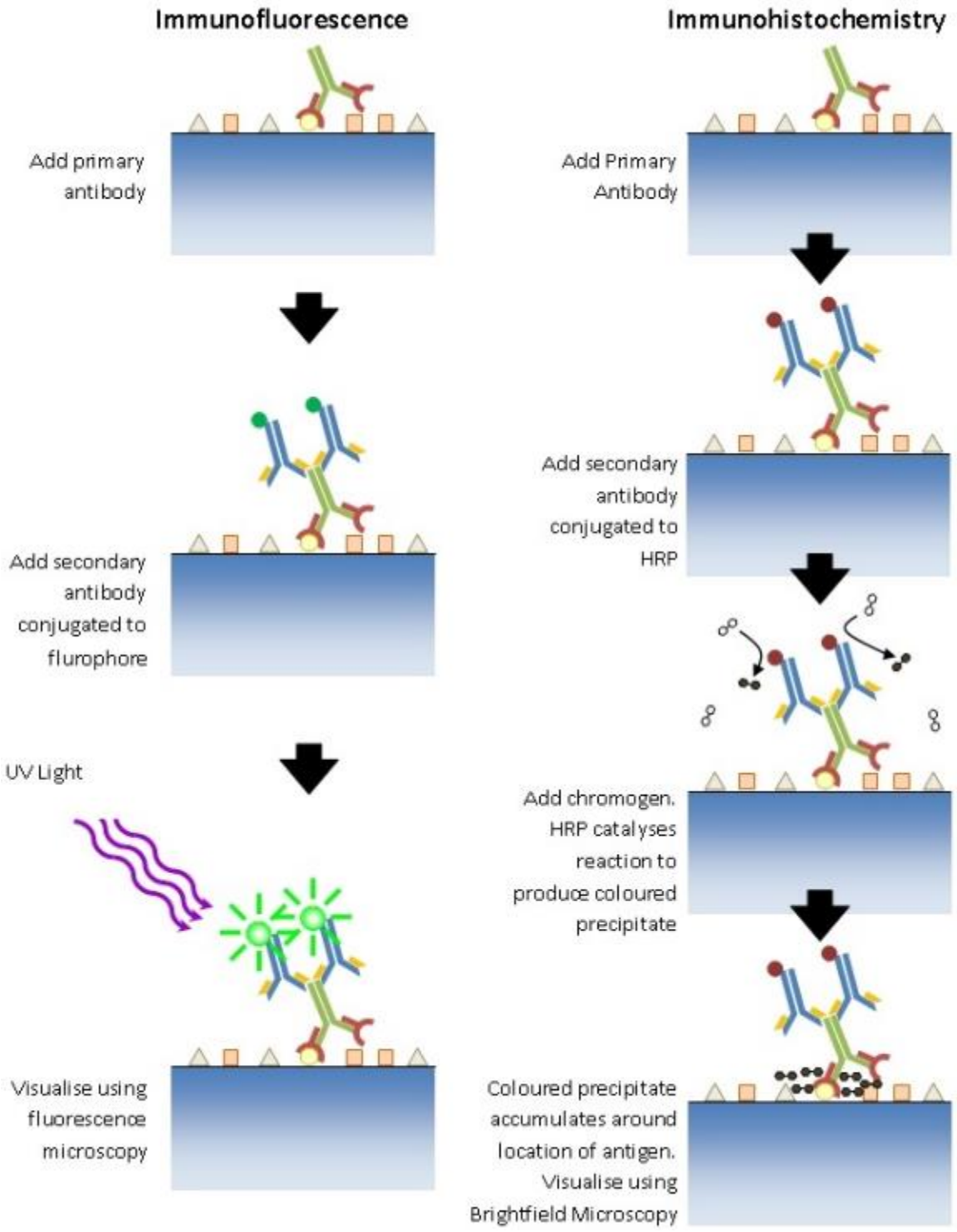

Figure 6: Figure showing two main types of IHC, immunofluorescence and substrate based detection. Both are commonly used (adapted from University of Queensland Diamantina Institute).

An antigen retrieval step will dissolve these cross-links, making it much easier for the antibodies to bind to the target antigen. Endogenous enzymatic activity that could act on the substrate dye must be blocked, in addition to any endogenous antigens that could bind antibodies that aren't the target, creating a noisy, hard-to-differentiate image. Next, depending on the imaging type (fluorescent vs enzymatic, for example), an enzyme-bound secondary antibody is used to bind to the first (primary) antibody, increasing the signal level for each antigen. If a secondary antibody is not needed, such as in fluorescent staining, the counterstain step can be proceeded to. The secondary antibody often has an enzyme conjugated to it, which will act on the dye substrate, producing color that is either visible in visual light or fluoresces at the locations of the antigen in the tissue. A counterstain is commonly needed to increase contrast. The sample is then dehydrated through an alcohol gradient, and mounted with a coverslip for imaging.

Developing an IH protocol for a new antigen requires considering multiple variables, such as the binding strength of the antibody to what buffer is used to rinse sections. The tissue sample must first be fixed (cross-linking to hold the tissue together after dehydration), decalcified if bone (hard tissues will pit the microtome blade/tear through sections), and cut with a microtome to between 5-10 micrometers thick. It must be thin in order to image via optical imaging.

Antigen retrieval is another important step, without it the antigen can be completely isolated from antibodies due to blocking via the cross-linking of the fixing process. There are two main types of antigen retrieval, enzyme based and heat based. Heat based antigen retrieval uses a weak acid or base solution to break down cross-linking, ideally without degrading the antigen. Enzyme based antigen retrieval is similar,

except is uses an enzyme such pepsin (derived from animals) to degrade the cross-linking. Unfortunately, there is not a generalized procedure that is applicable to all antigens, requiring individual tuning for the study of each antigen.

The most important ratio to consider when conducting an IHC experiment is the intensity of the background staining versus the target antigen staining. There several variables that can be changed to get high target staining while minimizing background staining. The first is blocking, in which serum from the primary/secondary antibody is used to minimize non-specific binding. The second is changing the antibody solution concentration. Tuning the antibody concentration during the primary incubation will allow for complete binding to the antigen (or primary antibody), while minimizing non-specific binding. Non-specific binding can be caused by cross-reactivity to other antigens in the sample, or simply antibodies becoming trapped in the structure of the tissue.

NOTE: SEE APPENDIX FOR SPECIFIC IHC PROTOCOLS

Chapter 3: Results

3.1 Nano-biomechanical Properties of WT Murine Knee Joint in PTOA Model

The modulus is a material property indicating the stiffness or stress-strain relationship of material or tissue. Previous studies have measured healthy murine articular cartilage to have a modulus of approximately 1.5 to 1.8 MPa [29]. The modulus changes were measured via Nanoindentation 2 and 8 weeks after induced PTOA model by destabilization of the medial meniscus (DMM surgery). The right hind knee was used for DMM, Sham was contralateral to DMM knee. On the Sham knee, as expected, cartilage retained a consistent modulus range throughout the tested time frame. The DMM cartilage modulus declined to 35 ± 12% and 22 ± 6% of the Sham control at 2 and 8 weeks post-surgery, respectively.

As expected, during the progression of DMM-induced PTOA, cartilage exhibits significantly lower modulus on the DMM-operated knees when compared to the contralateral Sham knees. In the 2 week post-surgery samples, only the medial section of the cartilage had a statistically significant difference when compared to the medial sham cartilage. At 8 weeks, however, both the medial and lateral DMM cartilage tissues were significantly reduced compared to the sham samples. There was no significant difference between 2 and 8-week sham samples, including comparing the medial and lateral cartilage sections. Figure 7 shows **intra**-time point comparisons while figure 8 shows **inter**-time point comparisons. Refer to tables 2 and 3 for tested statistical comparisons and *p*-values

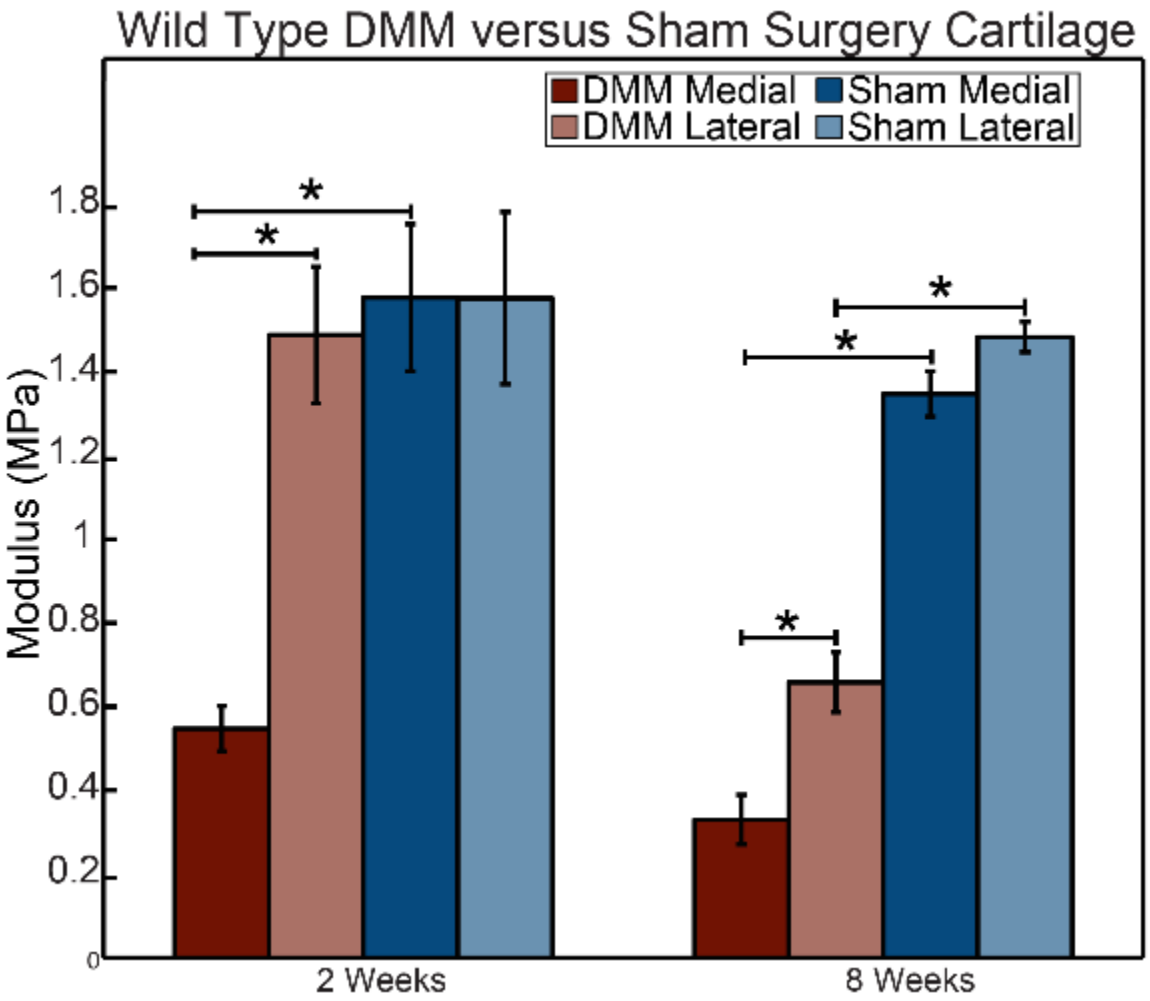

Figure 7: Nanoindentation modulus values of wild type mouse post-DMM and post-Sham surgery cartilage. The medial and lateral sections of tibia cartilage were the regions indented on to obtain the modulus values. In this case, each time point was compared within its own values to determine significance between measurements of the same time point.

Table 2: Intra-cartilage sample comparisons and their respective p-values from 2-sided Student's T-Test. Statistically significant results are highlighted in green.

Intra-Time Point Modulus Comparisons

Time Point	Comparison	p-value	Conclusion
2 Weeks Post Surgery	DMM Medial vs. DMM Lateral	0.0006	Significant
	DMM Medial vs. Sham Medial	0.0005	Significant
	DMM Lateral vs. Sham Lateral	0.7699	Not Significant
8 Weeks Post Surgery	DMM Medial vs. DMM Lateral	0.0078	Significant
	DMM Medial vs. Sham Medial	< 0.0001	Significant
	DMM Lateral vs. Sham Lateral	< 0.0001	Significant

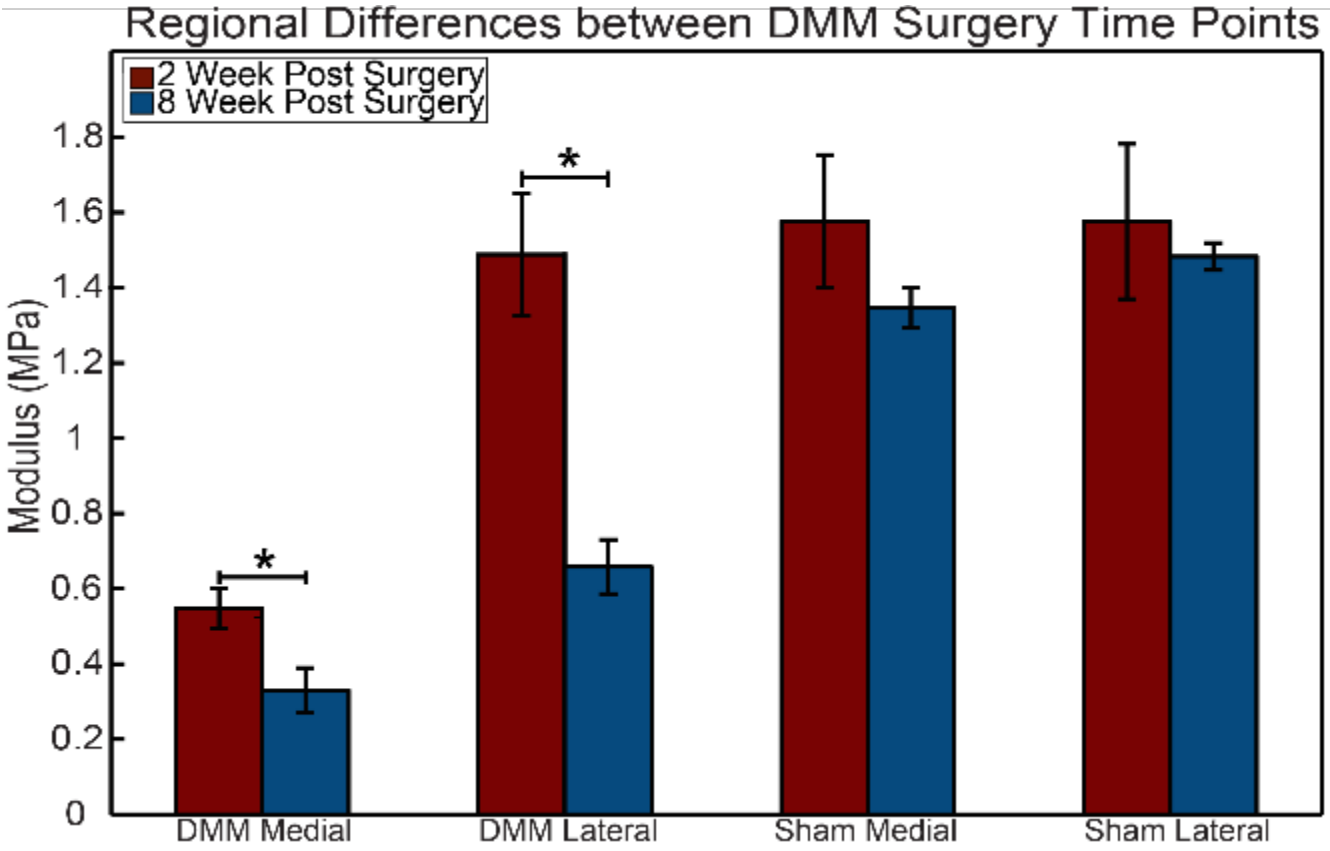

Figure 8: Inter time point modulus comparisons between 2 and 8 week post-DMM and post-sham cartilage samples. Samples of the same type for each time point were compared to see the development of changes to cartilage modulus.

Table 3: Inter-cartilage sample comparisons and their respective p-values from 2-sided Student's T-Test. Statistically significant results are highlighted in green. There was difference between each cartilage region for the different time points.

Inter-Time Point Modulus Comparisons

Cartilage Type	Comparison	p-value	Conclusion
DMM Medial	2 Weeks vs. 8 Weeks	0.0270	Significant
DMM Lateral	2 Weeks vs. 8 Weeks	0.0016	Significant
Sham Medial	2 Weeks vs. 8 Weeks	0.2487	Not Significant
Sham Lateral	2 Weeks vs. 8 Weeks	0.6974	Not Significant

Table 4: Raw data values of cartilage modulus for different regions, time points, and surgery types. Each modulus is measured in MPa, and are used in figures 7 and 8 above.

Cartilage Region	Time Point (Post Surgery)			
	2 Weeks		8 Weeks	
	Mean Modulus (MPa)	S.E.	Mean Modulus (MPa)	S.E.
DMM Medial	0.547 (N=10)	0.054	0.330 (N=10)	0.059
DMM Lateral	1.488 (N=5)	0.163	0.658 (N=5)	0.072
Sham Medial	1.577 (N=10)	0.176	1.347 (N=10)	0.054
Sham Lateral	1.567 (N=5)	0.206	1.483 (N=5)	0.036

3.2 Biomechanical Properties of Genetic Knockout Knee Joint in PTOA Model

Another modulus comparison was made between Wild-type mice and Decorin-null mice. Decorin is an important linker protein in the cartilage matrix, and is involved in binding Aggrecan to collagen, in addition to binding collagen types together. It is hypothesized that DCN-null mice will have a less organized and rigid matrix, resulting in softer (modulus-wise) matrix. Both cartilage types were indented on in the same fashion as above, with a comparison between WT and DCN (decorin) null mice.

Decorin-null mice were significantly softer than their equivalent wild-type samples, both in DMM and sham samples. . Interestingly, the difference between wild-type and decorin-null mice is larger (66% decrease in modulus), compared to in DMM

(54% decrease in modulus). Refer to tables 5 and 6 for tested statistical comparisons and *p*-values

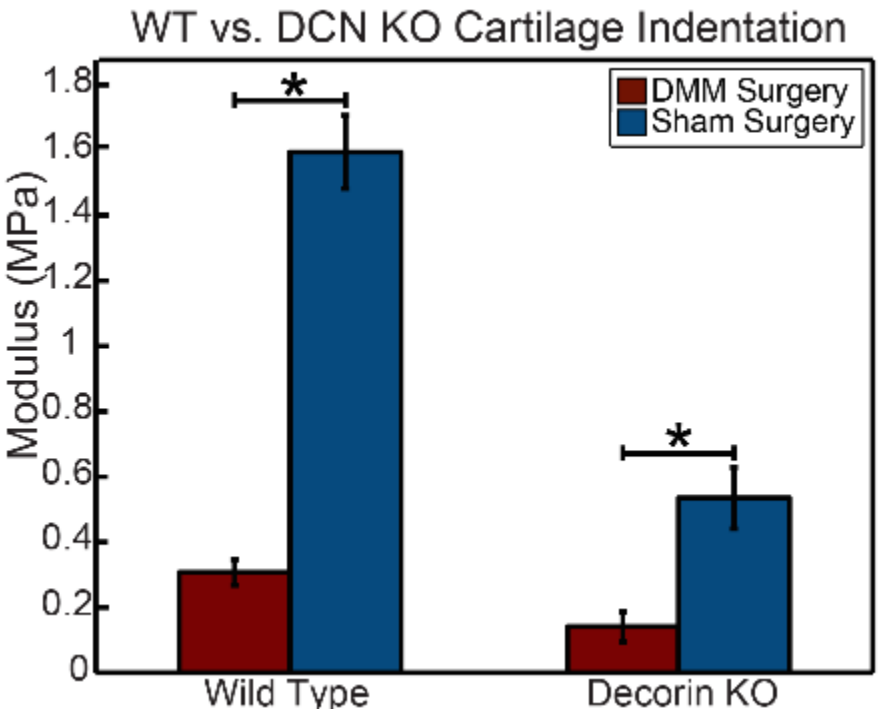

Figure 9: Intra-genotype modulus comparisons of WT and DCN-null mice. Both comparisons were significant as shown in Table 5.

Table 5: Significance comparisons made for intra-genotype modulus values, and each ones corresponding p-value. There was less of a difference when comparing DMM and Sham in DCN-null mice compared to the same comparison in WT mice.

Genotype	Comparison	p-value	Conclusion
Wild Type	DMM Surgery vs. Sham Surgery	< 0.0001	Significant
Decorin KO	DMM Surgery vs. Sham Surgery	0.0056	Significant

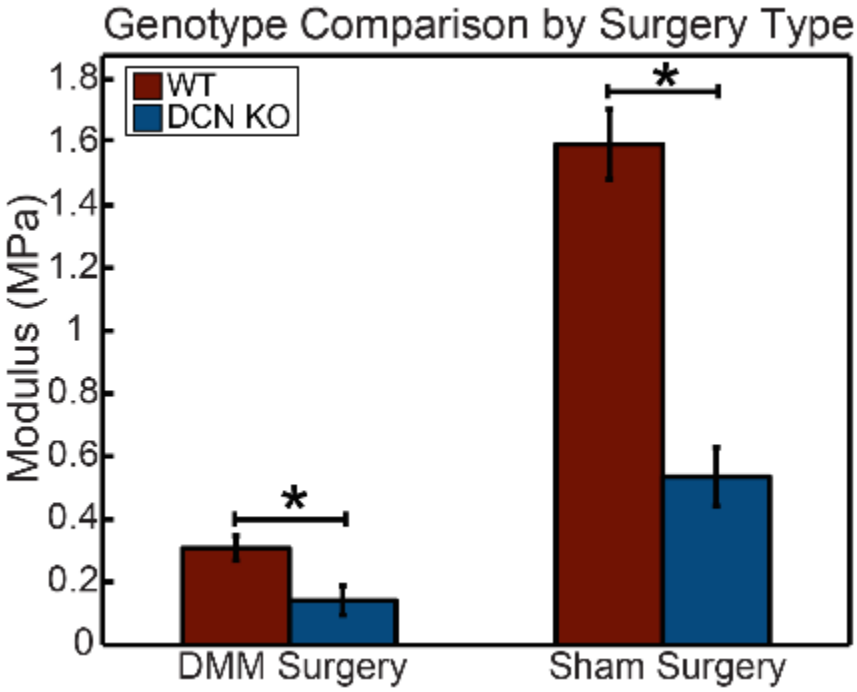

Figure 10: Inter-genotype modulus comparisons between WT and DCN-null murine surgery samples. The difference between the DMM samples is much smaller when compared to the difference in Sham samples.

Table 6: Comparisons and corresponding p-values of intra-surgery type modulus values.

Surgery Type	Comparison	p-value	Conclusion
DMM Surgery	Wild Type vs. Decorin KO	0.0227	Significant
Sham Surgery	Wild Type vs. Decorin KO	< 0.0001	Significant

Table 7: Raw data values used in Figure 9 and Figure 10.

Cartilage Type	Mouse Genotype			
	Wild Type		Decorin Knockout	
	Mean Modulus (MPa)	S.E.	Mean Modulus (MPa)	S.E.
DMM Surgery	0.307 (N=10)	0.039	0.141 (N=5)	0.046
Sham Surgery	1.594 (N=10)	0.112	0.535 (N=5)	0.094

3.3 Biochemical Signatures of Wild-Type PTOA Murine Model

3.3.1 BMP2 and pSmad1/5/8 staining in Wild Type DMM and Sham Sections

Two important biomarkers of PTOA were selected to be stained for in post-surgery murine cartilage sections. First, BMP2, is an important protein that stimulates chondrocyte matrix growth, but also increases metalloproteinase-13 (MMP-13) production [30]. MMP-13 breaks down the cartilage matrix by degrading both collagen and aggrecan core protein in PTOA. The second, pSmad1/5/8 is a down-stream intra-cellular messenger protein for BMP2, as well as transforming growth factor beta (TFG-beta) [31]. TGF-beta, much like BMP2, is involved in the catabolic and anabolic homeostasis in cartilage [31], and its deregulation can lead to cartilage degradation in OA and PTOA.

BMP2 and pSmad1/5/8 were up-regulated in post-surgical DMM murine cartilage compared to Sham cartilage. More specifically, DMM sections had the highest increase in BMP2 and pSmad1/5/8 in cartilage regions adjacent to the medial meniscus, which was destabilized in the DMM surgery. Anterior cartilage staining of both signaling proteins was higher than posterior, giving indication that the cartilage breakdown starts in the medial-anterior section of the knee after DMM surgery.

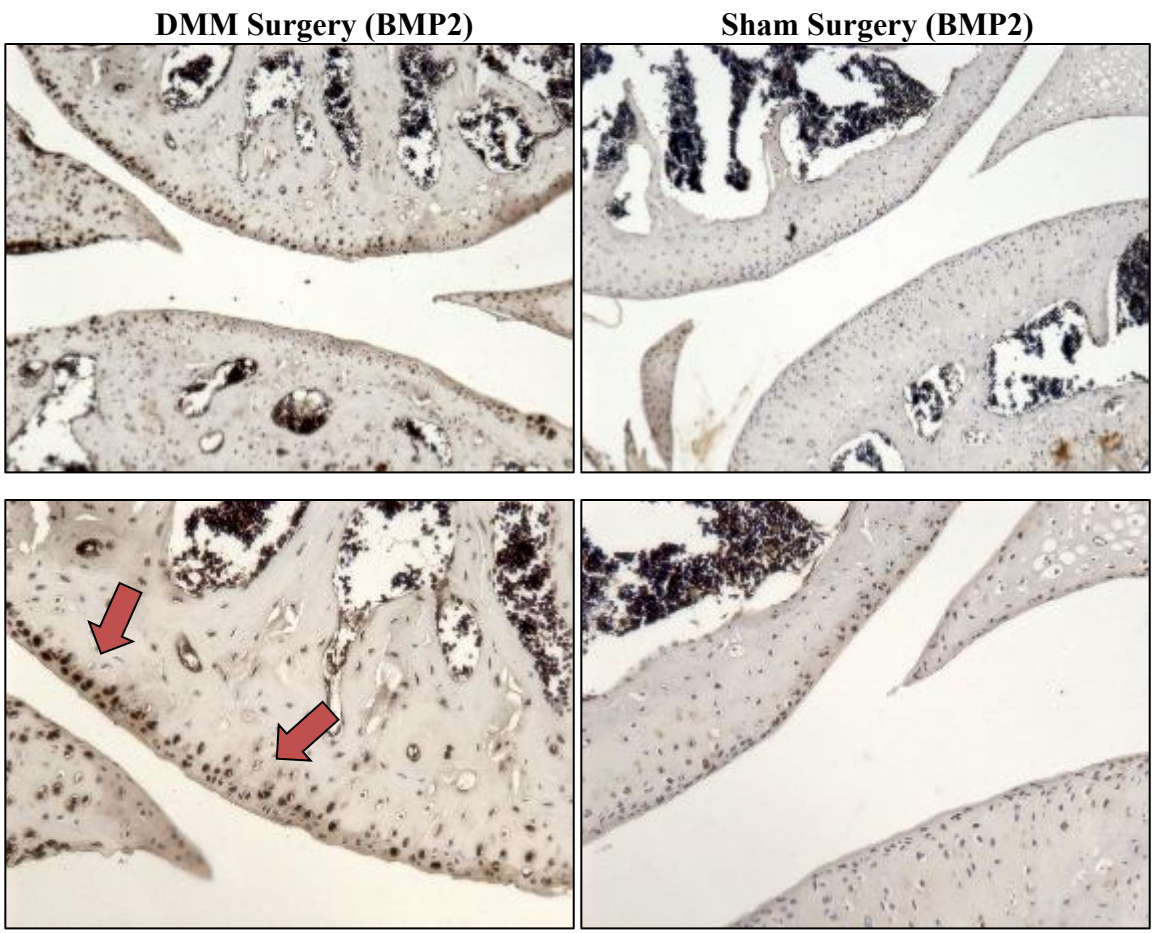

Figure 11: Representative IHC images showing up regulation of BMP2 antigen compared between DMM and Sham sections of murine cartilage. This is 8 weeks post-surgery. DMM are left images, Sham is right. All proceeding IHC staining is done with DAB brown (stain), with dark blue hematoxylin counterstain. Arrows are used to indicate sections of strong cartilage staining. Note: Top Images are shot at 10X, with bottom images shot at 20X.

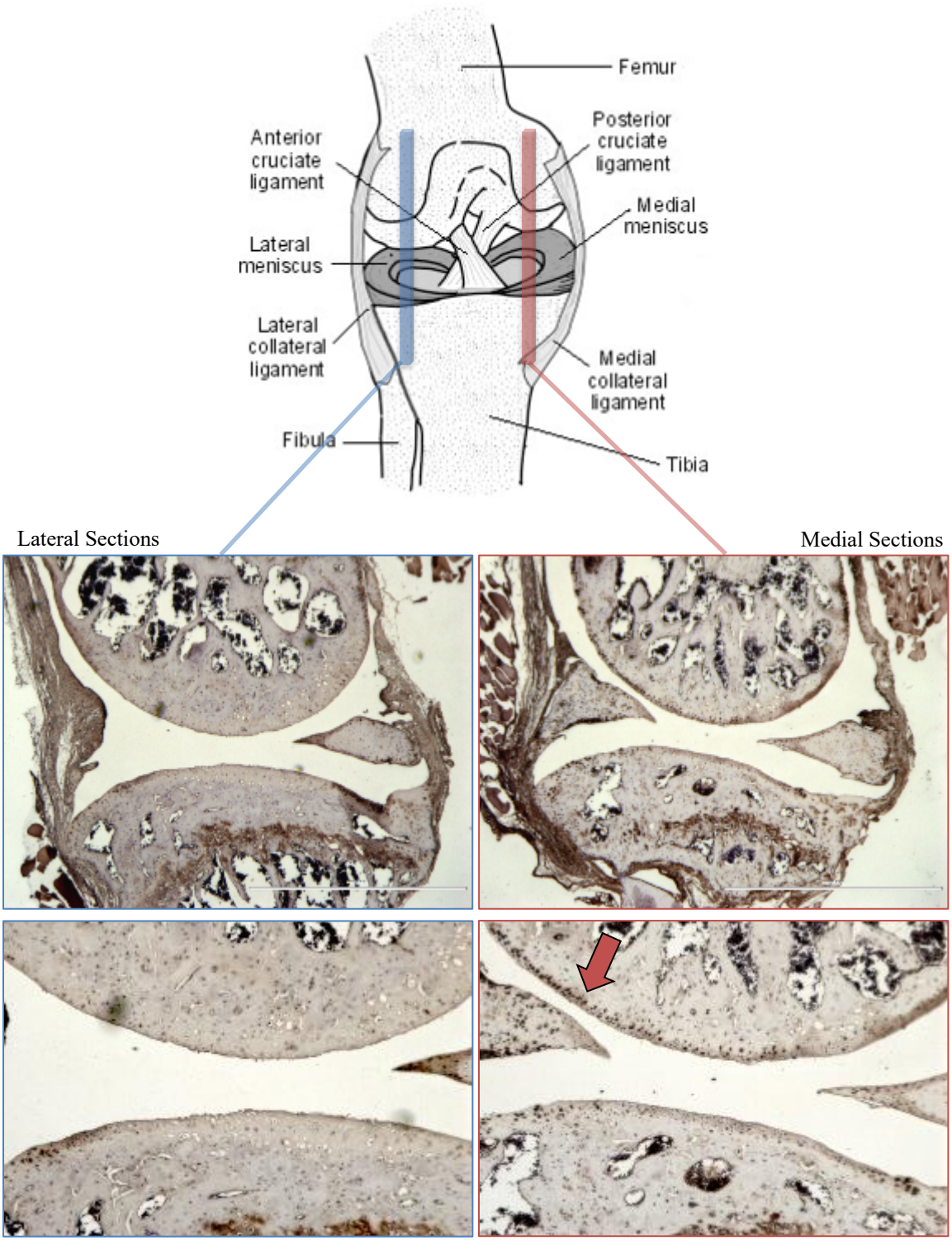

Figure 12: Figure showing increase in BMP2 expression in representative medial DMM sagittal sections compared to lateral DMM sections. Note increase is highest near medial meniscus on femoral cartilage of joint. Note: femur is top part of image, tibia is bottom. Additionally, middle images are 4X while bottom images are 10X. (Top diagram adapted from patient.info)

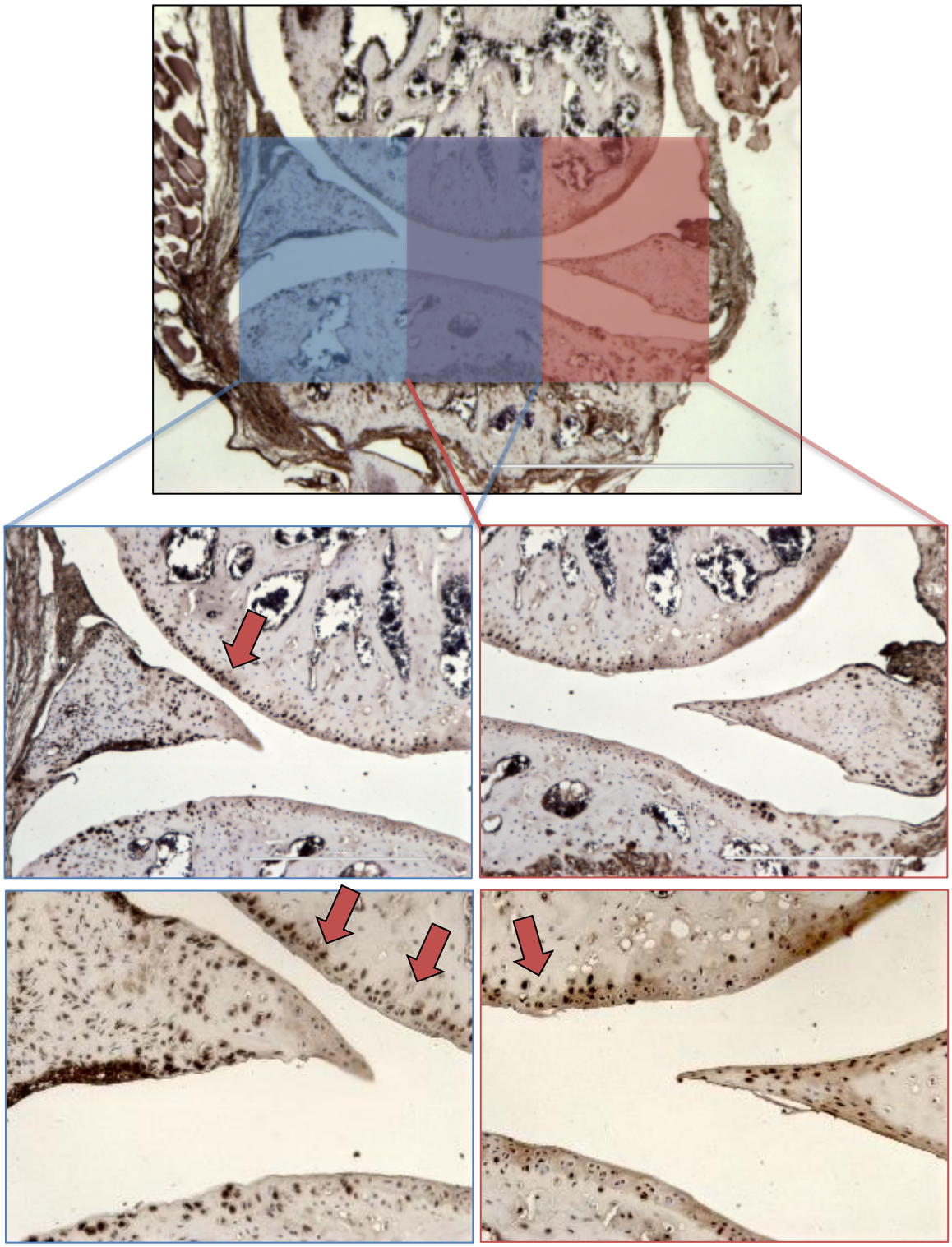

Figure 13: Regional difference of BMP2 staining between anterior and posterior areas of representative murine cartilage sections. There is increased staining on anterior part above the meniscus, compared to the posterior part above the meniscus. Top image is 4X, middle are 10X, and bottom are 20X.

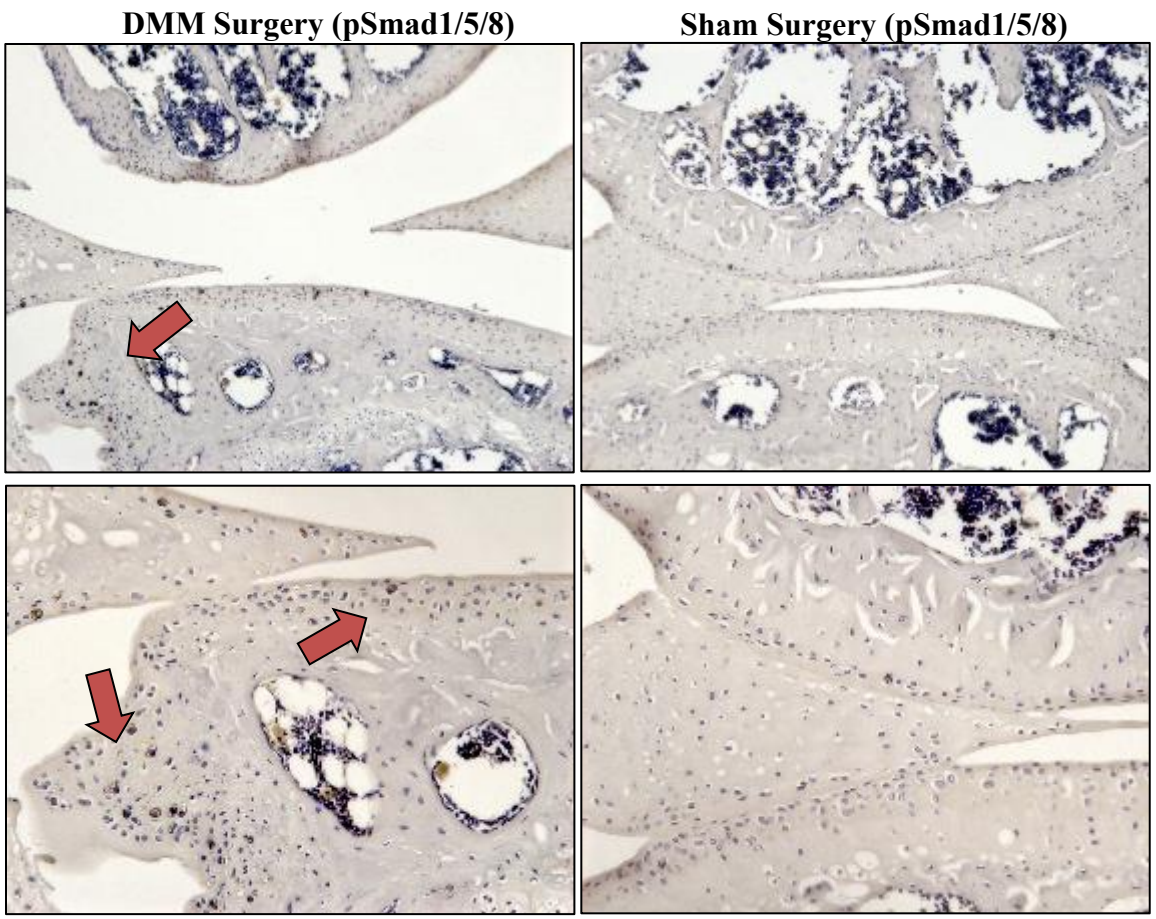

Figure 14: Representative IHC images showing up regulation of pSmad1/5/8 antigen compared between medial DMM and Sham sections of murine cartilage, 8 weeks post-surgery. Anterior of knee is left of each image. DMM are left images, Sham is right. There is not a lot of extracellular, staining,

since pSmad1/5/8 is intracellular. There is still slight increase in staining comparing DMM to Sham. Although not completely consistent with the BMP2 results, it is possible that BMP2 is using another signaling pathway. PSmad1/5/8 is also an intracellular messenger for TGF-beta, as mentioned above.

3.3.2: Aggrecan Expression in WT DMM Surgery and Sham Surgery Murine Cartilage

In addition to the signaling proteins BMP2 and pSmad1/5/8 mentioned above, aggrecan was also stained for in murine cartilage to examine expression. Aggrecan provides a hydrated gel-like property that gives cartilage its load bearing properties. It is a proteoglycan, and in common with all proteoglycans it possesses a core protein with covalently attached sulfated glycosaminoglycan (GAG) chains [32]. Aggrecan has a large number of extremely negatively charged glycosaminoglycan, allowing for a large binding of water, thereby reducing water flow in cartilage. Loss of aggrecan would result in a much decreased elasticity modulus, as shown above in the biomechanical section.

The reduction of aggrecan expression towards the superficial layer of cartilage corroborates the loss of structural homogeneity as shown in the biomechanical results section of this thesis. The loss of aggrecan was highest in the surface areas of the cartilage.

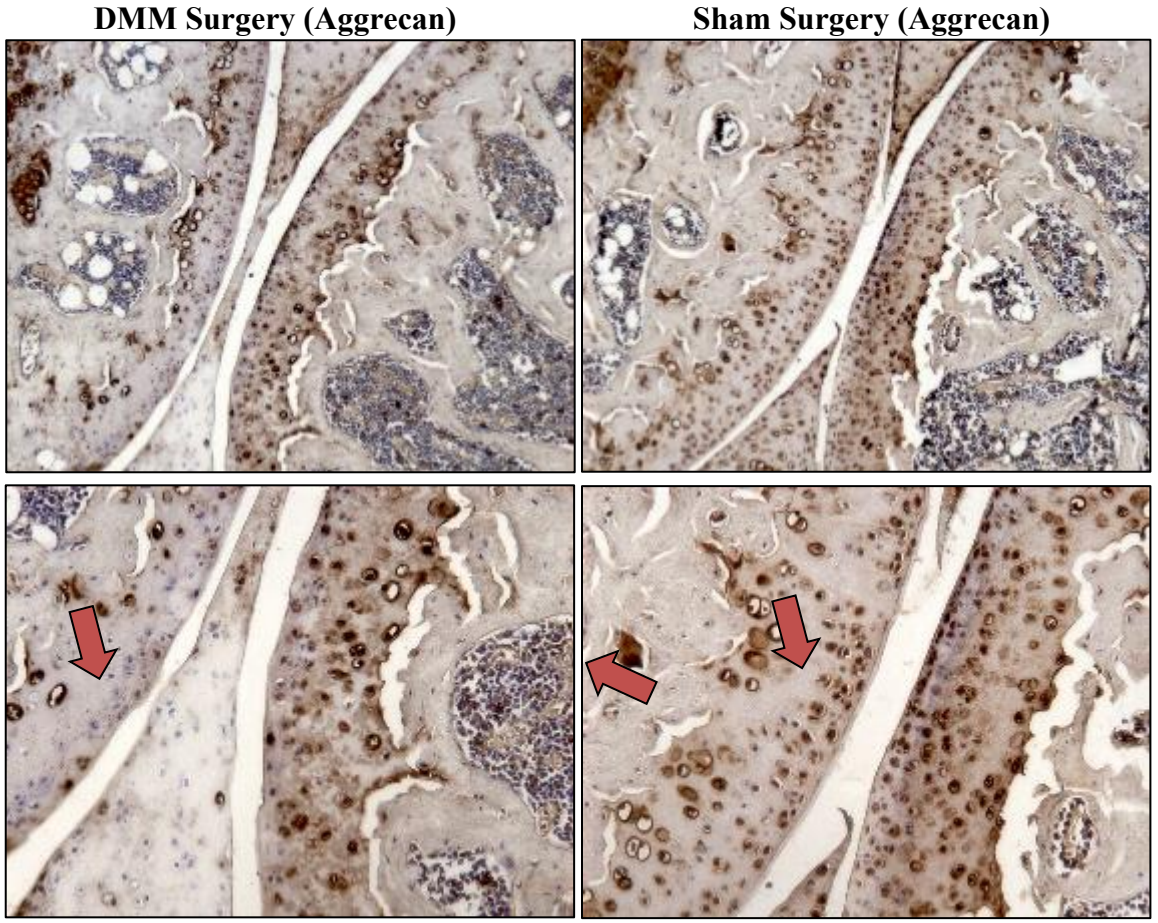

Figure 15: Aggrecan staining in DMM and Sham sagittal murine sections. There is a reduction of staining near cartilage surface in DMM compared to Sham, in addition to there being less staining overall. Refer to red arrows for areas with severely reduced aggrecan staining.

3.4 Exploring Matrix Changes of Decorin-null Murine Model

Decorin is an important matrix-regulating protein that is involved with binding both collagen and aggrecan in the cartilage matrix. Specifically, decorin is a regulatory protein that connects aggrecan to the collagen network (collagen types 2 and 6) in the ECM of cartilage [33].

In cartilage sections from one-month old (P30) decorin-null mice, there was a different in overall staining pattern in addition to expression levels when comparing to age-matched wild-type cartilage. Although a more quantitative method is required to remark if there is an overall difference in aggrecan amount between the two genotypes, we can see a difference in location of aggrecan between the two. Aggrecan in the decorin-null sections tends to be closer to the cartilage surface, while aggrecan in representative wild-type sections is more evenly distributed throughout the entirety of the cartilage. Additionally, there is a significant difference in the overall thickness of the cartilage, with the decorin cartilage layer being noticeably thinner than the Wild Type cartilage.

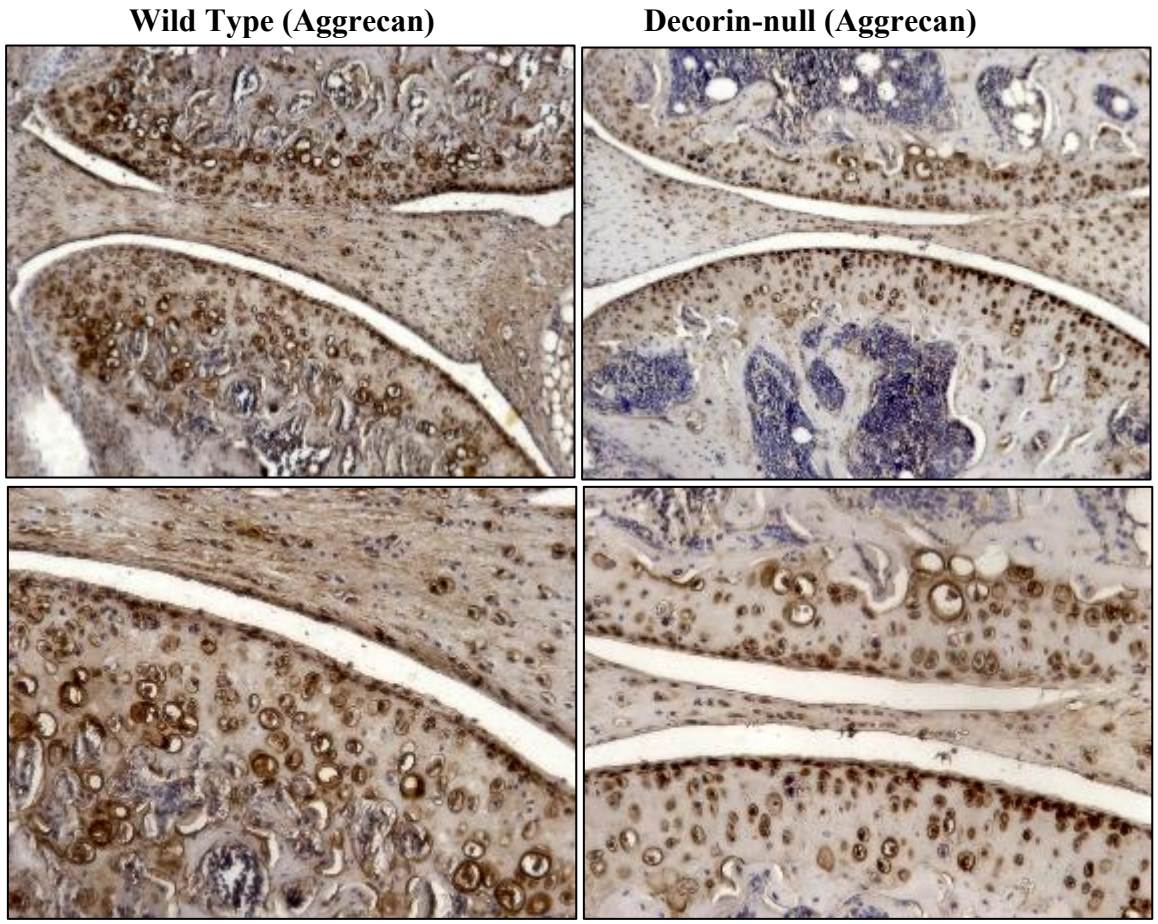

Figure 16: Staining patterns of aggrecan antibodies on both Wild Type and Decorin –Null Murine sections. There is a difference in staining pattern between the two, with more aggrecan being located closer to the cartilage surface in the Decorin-null sections. Although it seems that there is more aggrecan in the Wild-Type sections, a more quantitative approach should be used as the difference cannot be quantified in IHC. DAB substrate used as stain (brown), with hematoxylin (blue) used as counterstain for nuclear material. Top images are 10X, and bottom images are at 20X.

Chapter 4: Discussion

4.1: Mechanical and Chemical Changes after DMM Surgery

The reduction in effective nanoindentation modulus, E_{ind}, was shown to markedly precede histological signs on the medial side. In another study, Han Lab Group reported that at 1 week post-surgery, an earlier time than noticeable histological changes, modulus of the DMM knee cartilage was significantly reduced. Since cartilage mechanical properties are an integrated contribution of the matrix biochemical composition and structural organization [34], they can be influenced by both compositional and structural changes of cartilage extracellular matrix (ECM) at the molecular level. Aggrecan fragmentation and collagen fibril disorganization in the superficial layer are characteristic molecular events of early OA [35]. Such molecular changes can lead to the observed modulus reduction, but does not result in appreciable gross-level histological symptoms.

There is a statistically significant decrease in cartilage modulus at both 2 weeks and 8 weeks post DMM when compared to the contralateral sham procedure. This signifies that matrix degradation occurs quantifiably after injury. The DMM cartilage modulus declined to 35 ± 12% and 22 ± 6% of the Sham control at 2 and 8 weeks post-surgery, respectively. There are several reasons for the differences between the two surgery types.

Injury to cartilage induces an inflammatory response that disrupts normal chondrocyte function [9], either through immediate cell death due to injury or apoptosis-

inducing cytokines [9],[10], which act on a slower time scale. This change in chondrocyte behavior leads to inflammation-like catabolic changes to the matrix, leading to a loss in proteoglycans, in this case aggrecan. The loss of these charged matrix molecules results in a net increase of hydraulic permeability [36] in the cartilage, reducing DMM cartilage effective modulus. Water "migration" out of the cartilage could have an effect on the synovial fluid composition after hemarthrosis has decreased. A decreased lubricin concentration (an important lubricating protein found in synovial fluid) has been correlated with increases in markers of joint inflammation [37]. This destabilization of the medial meniscus reduces the stabilizing support of the medial meniscus between the femur and tibia, resulting in increased friction along both articular surfaces. This friction causes damage to the cartilage surface, resulting in OA-like lesion formation [22]. Disruption of the cartilage surface via lesions or otherwise is the first part of matrix degradation, as progressive layers are exposed to the frictional forces of the joint space over time.

One of the most reported matrix level differences after cartilage injury is a reduction of proteoglycans [9],[10],[11]. In the WT murine after DMM model, there is a significant difference in staining in aggrecan, in primarily superficial layers. This could be further examined to study if there was a pattern to location of the aggrecan loss.

In addition to the changes in aggrecan, differences in the signaling proteins BMP2 and its downstream facilitator pSmad1/5/8 in murine sections were also reported. BMP2 is a primarily beneficial signaling protein, inducing both matrix production and degradation [38]. It is worthy to note that, BMP2 is found at low levels in healthy cartilage, and is overexpressed in osteoarthritic cartilage [38]. An increased level of

BMP2 implies a change in the homeostasis of the normal anabolic and catabolic processes of cartilage. One hypothesis is that inflammatory cytokines and enzymes such as MMP13 break down the cartilage ECM, while another process reduces the proteoglycan synthesis to replace the loss, resulting in a net reduction of proteoglycan content as the cartilage degrades. The increase in pSmad1/5/8 is a bit more complicated, as it involved in multiple upstream signaling protein chains other than BMP2. For example, TF3G-beta 1 is another molecule that stimulates proteoglycan synthesis and is involved with the pSmad1/5/8 pathway. The increased intracellular pSmad1/5/8 as found in DMM versus sham sections further shows the loss of normal cartilage homeostasis, as both BMP2 and TGF-beta 1 are found at low levels in normal cartilage [38].

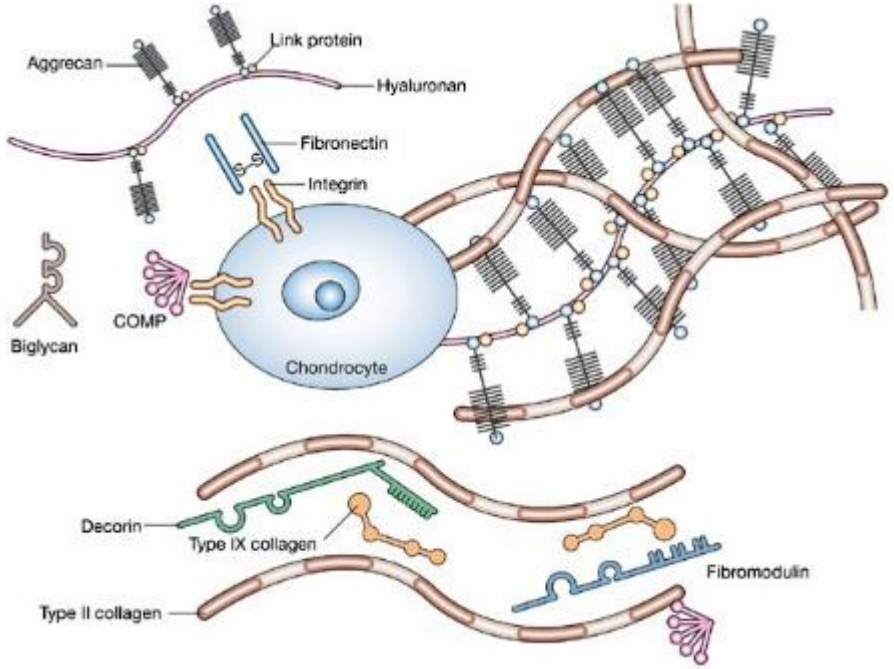

Figure 17: Extracellular matrix in cartilage surrounding an individual chondrocyte. Note how aggrecan is found to hyaluron, which is often connected to the collagen network via Decorin and other firbromodulins such as biglycan. This has implications for the Discussion section 5.3 as well. Image adapted from [39].

Although BMP-2 has potent anabolic actions, BMP activity in in murine cartilage was shown to induce OA-like changes by stimulation of MMP-13, directly favoring cartilage loss [30].

After injury, the amount of chondrocyte hypertrophy (terminal differentiation) lead to enhanced metabolic activity, changing the cartilage homeostasis to increase the amount of degeneration. As more hypertrophic chondrocytes develop, calcification and ossification will occur in portions of the cartilage that have not already degraded into OA. Inflammatory cytokines have a role in prompting chondrocytes to terminally differentiate as well [40].

In cartilage, chondrocytes are related to osteophytes, which control bone homeostasis and production. Initially during development, bone begins as cartilage, and as the organism develops, the terminal differentiation of chondrocytes towards a more osteophyte-like phenotype is blocked to allow for mature hyaline cartilage. One hypothesis for the development is that injury to cartilage initiates this terminal differentiation of chondrocytes [40], eventually resulting in ossification of the cartilage, similar to that during development. This occurs during the breakdown of the matrix as well, resulting in degrading and eventual hardening of cartilage that is the long-term outcome of post-traumatic osteoarthritis.

4.2: Spatiotemporal Progression of PTOA in wild-type Model

Significant modulus reduction of cartilage on the lateral side was measured at 8 weeks after DMM, later than the directly injured medial side. Since DMM directly affects the loading on the medial side, it is expected that lateral cartilage degradation, if present, is moderate. Here, nanoindentation results clearly illustrate the presence of spatiotemporal progression of OA from the medial to the lateral side, highlighting the whole joint nature of OA. Such changes are due to altered loading pattern on the lateral side after DMM, elevated catabolic enzymatic activities in the joint capsule, as well as altered lateral side cartilage contact mechanics upon the degradation of medial cartilage[41].

BMP2 was over-expressed in the medial section of cartilage compared to that of the lateral as well. BMP2 is a signaling protein that induces cartilage matrix remodeling and is generally viewed as beneficial, but is still part of the matrix homeostasis that must be maintained in healthy cartilage [38]. The increased level of BMP2 staining in medial sections of post-DMM cartilage implies a change in this homeostasis. Glasson et al noted the development of cartilage lesions on the anterior central region of the joint [22]. This has some implications, as the cartilage is initially damaged close to the surgical site, at the medial side of the joint. The damage cycle will begin at this area, and propagates itself to eventually effect areas further away in the same joint. Inflammatory cytokines play a major role, and surface friction cause additional damage to adjacent cartilage. Finally, the reduced level of lubricating proteins in the synovial fluid could affect the whole joint, as a result of bleeding at the initial surgical site. Targeting a single injury

region in cartilage via pharmacological solutions could stop this propagation of damage to the rest of the joint. Although it would have to be done immediately after injury in order to block the spatio-temporal progression of OA.

4.3: The Role of Decorin in stabilizing the Extra-Cellular Matrix of Murine Cartilage

Decorin-null mice experience significant changes in nano-mechanical properties in both DMM and Sham surgeries. The difference between wild-type and decorin-null mice is larger (66% decrease in modulus), compared to in DMM (54% decrease in modulus). Aggrecan in the decorin null mice is also located closer to the articular cartilage surface than it is in the equivalent age Wild Type mice. Decorin binds aggrecan to hyaluronic acid and the collagen matrix [33]. Although there are other regulatory ECM proteins such as biglycan, one possibility is that new aggrecan synthesized to replace those broken down after injury are not able to bind to the cartilage matrix, resulting in the eventual migration of proteoglycans out of the cartilage itself. An experiment could easily test for aggrecan levels in the synovial fluid of Wild Type versus decorin null mice after DMM surgery to examine this possibility.

On a more general level, decorin has an important regulatory role in the cartilage matrix. The loss of decorin results in a reduction in the overarching structural order of cartilage. This conclusion is backed by the sham decorin-null cartilage having a significantly softer indentation modulus than that of Wild Type after the DMM surgery. Decorin plays a collagen-related role in many different parts of the body, including skin. An example of this regulatory importance is in keloid scars in skin, which have a reduced

amount of decorin compared to healthy skin [42]. Another possibility for the changes in modulus in the DCN-null mice cartilage is that collagen is not as organized, resulting in a reduced ability to adapt to forces induced on the cartilage surface.

At its most basic level, post-traumatic osteoarthritis is a joint injury that causes biochemical and biomechanical changes to the cartilage of that injured joint. More specifically, PTOA causes irreparable changes to cartilage chondrocytes and the cartilage matrix. Understanding the complex mechanism by which these changes occur is important not only to treat existing cases of post-traumatic osteoarthritis, but also for preventing it.

Chapter 5: Conclusions

This thesis demonstrates the high sensitivity of nanoindentation modulus to the early stage degradation of cartilage in murine PTOA. The decrease of modulus at 2 weeks after DMM is attributed to the increased catabolic enzyme activities following the surgery. At the intermediate and late stage, progression of OA starts to influence the mechanics of lateral cartilage, indicating a spatio-temporal development of the disease. Aggrecan is reduced 8 weeks after DMM, and cartilage cytokines BMP2 and pSmad1/5/8 proteins increase in expression. Decorin also has an important regulatory role in normal cartilage, and decorin-null mice experience changes in both biochemical and biomechanical properties. DCN-null mice have changed aggrecan expression locations as well as statistically significantly lower indentation moduli when compared to aged-matched, equivalent wild-type murine cartilages.

The changes in biochemical and biomechanical properties of murine cartilage after DMM examined in this thesis grant some insights into the pathogenesis of OA in murine models. BMP2, commonly a marker of beneficial cartilage remodeling, is overexpressed in DMM cartilage compared to Sham. The ECM, in the form of aggrecan, breaks down after DMM as well, changing the nano-mechanical properties of both wild type and decorin null cartilages. The results provide important knowledge for the etiology of PTOA and the search of early detection and prevention strategies. The methods

presented here can be combined with other transgenic murine OA models to further elucidate the molecular etiology of PTOA.

Important follow-up studies for this research would be to examine a large spectrum of inflammatory molecules, signaling cytokines, and other biomarkers of chondrocytes in both healthy and surgically induced OA murine models. Additionally, furthur insight into the complicated ECM composition is needed to fully explain why mechanical changes of cartilage after DMM are apparent before any histological changes can be detected.

In the study of osteoarthritis, any one study is only a piece of the complicated structure and function of joint cartilage. Any kind of pharmacological solution to the cartilage degradation following joint injury has to take into consideration the complex homeostasis of cartilage. Additionally, consider that each and every patient has a slightly different level of the different indicators of PTOA. One patient may have elevated levels of IL-I or BMP2, but have no evidence of cartilage degradation, while another has "typical" levels but still has cartilage degradation following injury.

Although daunting, being able to prevent long-term cartilage damage following injury would help many people avoid a lifetime of pain and loss of mobility. Hopefully a small piece of the puzzle of PTOA has been examined with this thesis, granting some insight into matrix and chondrocyte changes following an induced injury in a murine model.

List of References

1. Anderson, D.D., S. Chubinskaya, F. Guilak, J.A. Martin, T.R. Oegema, S.A. Olson, and J.A. Buckwalter, *POST-TRAUMATIC OSTEOARTHRITIS: IMPROVED UNDERSTANDING AND OPPORTUNITIES FOR EARLY INTERVENTION.* Journal of orthopaedic research : official publication of the Orthopaedic Research Society, 2011. **29**(6): p. 802-809.

2. Buckwalter, J.A., *Articular cartilage: injuries and potential for healing.* J Orthop Sports Phys Ther, 1998. **28**(4): p. 192-202.

3. Buckwalter, J.A. and T.D. Brown, *Joint injury, repair, and remodeling: roles in post-traumatic osteoarthritis.* Clinical orthopaedics and related research, 2004. **423**: p. 7-16.

4. Brown, T.D., R.C. Johnston, C.L. Saltzman, J.L. Marsh, and J.A. Buckwalter, *Posttraumatic osteoarthritis: a first estimate of incidence, prevalence, and burden of disease.* Journal of orthopaedic trauma, 2006. **20**(10): p. 739-744.

5. Lohmander, L.S., A. Östenberg, M. Englund, and H. Roos, *High prevalence of knee osteoarthritis, pain, and functional limitations in female soccer players twelve years after anterior cruciate ligament injury.* Arthritis & Rheumatism, 2004. **50**(10): p. 3145-3152.

6. Von Porat, A., E.M. Roos, and H. Roos, *High prevalence of osteoarthritis 14 years after an anterior cruciate ligament tear in male soccer players: a study of radiographic and patient relevant outcomes.* Annals of the rheumatic diseases, 2004. **63**(3): p. 269-273.

7. Nordenvall, R., S. Bahmanyar, J. Adami, V.M. Mattila, and L. Felländer-Tsai, *Cruciate Ligament Reconstruction and Risk of Knee Osteoarthritis: The Association between Cruciate Ligament Injury and Post-Traumatic Osteoarthritis. A Population Based Nationwide Study in Sweden, 1987–2009.* PloS one, 2014. **9**(8): p. e104681.

8. Schenker, M.L., R.L. Mauck, J. Ahn, and S. Mehta, *Pathogenesis and Prevention of Posttraumatic Osteoarthritis After Intra-articular Fracture.* The Journal of the American Academy of Orthopaedic Surgeons, 2014. **22**(1): p. 20-28.

9. Lotz, M.K., *New developments in osteoarthritis: Posttraumatic osteoarthritis: pathogenesis and pharmacological treatment options.* Arthritis Research & Therapy, 2010. **12**(3): p. 1-9.

10. Sherwood, J.C., J. Bertrand, S.E. Eldridge, and F. Dell'Accio, *Cellular and molecular mechanisms of cartilage damage and repair.* Drug Discovery Today, 2014. **19**(8): p. 1172-1177.

11. Levin, A., N. Burton-Wurster, C.T. Chen, and G. Lust, *Intercellular signaling as a cause of cell death in cyclically impacted cartilage explants.* Osteoarthritis and Cartilage, 2001. **9**(8): p. 702-711.

12. Caramés, B., N. Taniguchi, S. Otsuki, F.J. Blanco, and M. Lotz, *Autophagy is a Protective Mechanism in Normal Cartilage and its Aging-related Loss is Linked with Cell Death and Osteoarthritis.* Arthritis and rheumatism, 2010. **62**(3): p. 791-801.

13. Hooiveld, M., G. Roosendaal, M. Wenting, M. van den Berg, J. Bijlsma, and F. Lafeber, *Short-Term Exposure of Cartilage to Blood Results in Chondrocyte Apoptosis.* The American Journal of Pathology, 2003. **162**(3): p. 943-951.

14. Marks, P.H. and M.L.C. Donaldson, *Inflammatory Cytokine Profiles Associated With Chondral Damage in the Anterior Cruciate Ligament–Deficient Knee.* Arthroscopy: The Journal of Arthroscopic & Related Surgery, 2005. **21**(11): p. 1342-1347.

15. Aigner, T., K. Fundel, J. Saas, P.M. Gebhard, J. Haag, T. Weiss, A. Zien, F. Obermayr, R. Zimmer, and E. Bartnik, *Large-scale gene expression profiling reveals major pathogenetic pathways of cartilage degeneration in osteoarthritis.* Arthritis & Rheumatism, 2006. **54**(11): p. 3533-3544.

16. Serra, R., M. Johnson, E.H. Filvaroff, J. LaBorde, D.M. Sheehan, R. Derynck, and H.L. Moses, *Expression of a Truncated, Kinase-Defective TGF-β Type II Receptor in Mouse Skeletal Tissue Promotes Terminal Chondrocyte Differentiation and Osteoarthritis.* The Journal of Cell Biology, 1997. **139**(2): p. 541-552.

17. Schiphof, D., M. Boers, and S.M.A. Bierma-Zeinstra, *Differences in descriptions of Kellgren and Lawrence grades of knee osteoarthritis.* Annals of the rheumatic diseases, 2008. **67**(7): p. 1034-1036.

18. Roos, E.M., *Joint injury causes knee osteoarthritis in young adults.* Current opinion in rheumatology, 2005. **17**(2): p. 195-200.

19. Foran, J.R.H. *Total Knee Replacement - AAOS*. 2015 [cited 2016 January 31].

20. Chubinskaya, S. and M.A. Wimmer, *Key Pathways to Prevent Posttraumatic Arthritis for Future Molecule-Based Therapy.* Cartilage, 2013. **4**(3 Suppl): p. 13S-21S.

21. Little, C.B. and D.J. Hunter, *Post-traumatic osteoarthritis: from mouse models to clinical trials.* Nat Rev Rheumatol, 2013. **9**(8): p. 485-497.

22. Glasson, S.S., T.J. Blanchet, and E.A. Morris, *The surgical destabilization of the medial meniscus (DMM) model of osteoarthritis in the 129/SvEv mouse.* Osteoarthritis and Cartilage, 2007. **15**(9): p. 1061-1069.

23. Glasson, S.S., M.G. Chambers, W.B. Van Den Berg, and C.B. Little, *The OARSI histopathology initiative – recommendations for histological assessments of osteoarthritis in the mouse.* Osteoarthritis and Cartilage, 2010. **18, Supplement 3**: p. S17-S23.

24. Ma, H.L., T.J. Blanchet, D. Peluso, B. Hopkins, E.A. Morris, and S.S. Glasson, *Osteoarthritis severity is sex dependent in a surgical mouse model.* Osteoarthritis and Cartilage, 2007. **15**(6): . 695-700.

25. Glasson, S.S., R. Askew, B. Sheppard, B. Carito, T. Blanchet, H.-L. Ma, C.R. Flannery, D. Peluso, K. Kanki, Z. Yang, M.K. Majumdar, and E.A. Morris, *Deletion of active ADAMTS5 prevents cartilage degradation in a murine model of osteoarthritis.* Nature, 2005. **434**(7033): p. 644-648.

26. Zhang, X., J. Zhu, F. Liu, Y. Li, A. Chandra, L.S. Levin, F. Beier, M. Enomoto-Iwamoto, and L. Qin, *Reduced EGFR signaling enhances cartilage destruction in a mouse osteoarthritis model.* Bone Research, 2014. **2**: p. 14015.

27. Han, L. and A.J. Grodzinsky, *Advances and Applications of Nanomechanical Tools in Cartilage Tissue Engineering*, in *A Tissue Regeneration Approach to Bone and Cartilage Repair*, H. Zreiqat, R.C. Dunstan, and V. Rosen, Editors. 2015, Springer International Publishing: Cham. p. 191-218.

28. Coons, A.H., H.J. Crrech, and R.N. Jones, *Immunological Properties of an Antibody Containing a Fluorescent Group.* Experimental Biology and Medicine, 1941. **47**(2): p. 3.

29. Batista, M.A., H.T. Nia, P. Önnerfjord, K.A. Cox, C. Ortiz, A.J. Grodzinsky, D. Heinegård, and L. Han, *Nanomechanical phenotype of chondroadherin-null murine articular cartilage.* Matrix Biology, 2014. **38**: p. 84-90.

30. Aref-Eshghi, E., M. Liu, P.E. Harper, J. Doré, G. Martin, A. Furey, R. Green, P. Rahman, and G. Zhai, *Overexpression of MMP13 in human osteoarthritic cartilage is associated with the SMAD-independent TGF-β signalling pathway.* Arthritis Research & Therapy, 2015. **17**(1): p. 264.

31. Shen, J., S. Li, and D. Chen, *TGF-β signaling and the development of osteoarthritis.* Bone Research, 2014. **2**: p. 14002.

32. Roughley, P.J. and J.S. Mort, *The role of aggrecan in normal and osteoarthritic cartilage.* Journal of Experimental Orthopaedics, 2014. **1**(1): p. 1-11.

33. Wiberg, C., A.R. Klatt, R. Wagener, M. Paulsson, J.F. Bateman, D. Heinegård, and M. Mörgelin, *Complexes of Matrilin-1 and Biglycan or Decorin Connect Collagen VI Microfibrils to Both Collagen II and Aggrecan.* Journal of Biological Chemistry, 2003. **278**(39): p. 37698-37704.

34. Hung, C.T. and G.A. Ateshian, *Grading of osteoarthritic cartilage: Correlations between histology and biomechanics.* Journal of Orthopaedic Research, 2016. **34**(1): p. 8-9.

35. Saarakkala, S., P. Julkunen, P. Kiviranta, J. Mäkitalo, J.S. Jurvelin, and R.K. Korhonen, *Depth-wise progression of osteoarthritis in human articular cartilage: investigation of composition, structure and biomechanics.* Osteoarthritis and Cartilage, 2010. **18**(1): p. 73-81.

36. Kiani, C., L. Chen, Y.J. Wu, A.J. Yee, and B.B. Yang, *Structure and function of aggrecan.* Cell Res, 2002. **12**(1): p. 19-32.

37. Elsaid, K.A., B.C. Fleming, H.L. Oksendahl, J.T. Machan, P.D. Fadale, M.J. Hulstyn, R. Shalvoy, and G.D. Jay, *Decreased Lubricin Concentrations and Markers of Joint Inflammation in Synovial Fluids from Patients with Anterior Cruciate Ligament Injury.* Arthritis and rheumatism, 2008. **58**(6): p. 1707-1715.

38. Davidson, E.N.B., E.L. Vitters, P.L.E.M. van Lent, F.A.J. van de Loo, W.B. van den Berg, and P.M. van der Kraan, *Elevated extracellular matrix production and degradation upon bone morphogenetic protein-2 (BMP-2) stimulation point toward a role for BMP-2 in cartilage repair and remodeling.* Arthritis Research & Therapy, 2007. **9**(5): p. R102-R102.

39. Chen, F.H., K.T. Rousche, and R.S. Tuan, *Technology Insight: adult stem cells in cartilage regeneration and tissue engineering.* Nat Clin Pract Rheum, 2006. **2**(7): p. 373-382.

40. van der Kraan, P.M. and W.B. van den Berg, *Chondrocyte hypertrophy and osteoarthritis: role in initiation and progression of cartilage degeneration?* Osteoarthritis and Cartilage, 2012. **20**(3): p. 223-232.

41. Temple-Wong, M.M., W.C. Bae, M.Q. Chen, W.D. Bugbee, D. Amiel, R.D. Coutts, M. Lotz, and R.L. Sah, *Biomechanical, Structural, and Biochemical Indices of Degenerative and Osteoarthritic Deterioration of Adult Human Articular Cartilage of the Femoral Condyle.* Osteoarthritis and cartilage / OARS, Osteoarthritis Research Society, 2009. **17**(11): p. 1469-1476.

42. Jumper, N., R. Paus, and A. Bayat, *Functional histopathology of keloid disease.* Histology and histopathology, 2015. **30**(9): p. 1033-1057.

Appendix A: Experimental Protocols

A.1: Generalized Immunohistochemical Staining Protocol for Paraffin-Embedded Murine Cartilage Sections

Han Lab
BMP2/pSmad1/5/8 Protocol Checklist
Day 1 – Working Time : 4.5 hours

Deparaffinize and Rehydrate Slides

- Bake slides at 60°C	30 min
- Xylene bath	5 min
- Xylene bath	5 min
- Xylene bath	5 min
- 100% ethanol bath	3 min
- 95% ethanol bath	3 min
- 95% ethanol bath	3 min
- 70% ethanol bath	3 min
- dH_2O bath	3 min
- dH_2O bath	3 min

Epitope Retrieval

- Slides into sealable container with NaCitrate Buffer	
- Place into water bath, set at 65°C	60 min
- Let cool at room temp.	20 min
- dH_2O bath	5 min
- dH_2O bath	5 min

IHC Endogenous Blocking

- Outline sections with PAP pen	
- Incubate sections with Dual Blocking Agent	30 min
- dH_2O bath	5 min
- dH_2O bath	5 min
- 1X PBST bath	5 min
- Incubate sections with Normal Goat Serum	30 min
- Incubate sections with Avidin Block	15 min
- 1X PBST bath	5 min
- 1X PBST bath	5 min
- Incubate sections with Biotin Block	15 min
- 1X PBST bath	5 min
- 1X PBST bath	5 min

Primary Incubation

- Incubate with primary antibody	overnight

Han Lab
BMP2/pSmad1/5/8 Protocol Checklist
Day 2 – Working Time : 3.25 hours

BMP2 Secondary Antibody and Avidin/Biotin Complex Formation

- Slides warm up to room temp	20 min
- 1X PBST bath	5 min
- 1X PBST bath	5 min
- 1X PBST bath	5 min
- 1X PBST bath	5 min
- 1X PBST bath	5 min
- Incubate with secondary antibody	30 min
- Create ABC reagent	
- 1X PBST bath	5 min
- 1X PBST bath	5 min
- 1X PBST bath	5 min
- 1X PBST bath	5 min
- 1X PBST bath	5 min
- Incubate with ABC reagent	30 min
- 1X PBST bath	3 min
- 1X PBST bath	3 min
- 1X PBST bath	3 min
- 1X PBST bath	3 min
- dH_2O bath	3 min
- dH_2O bath	3 min

DAB Substrate Timing, Counterstaining, and Mounting

- Incubate with DAB substrate	5 min
- Stop reaction with dH_2O bath, rinse with dH_2O	
- Stain in Mayer's hematoxylin	5 min
- Rinse with tap water	
- **PBS** bath	1 min
- Rinse with dH_2O bath	
- 70% ethanol bath	3 min
- 95% ethanol bath	3 min
- 95% ethanol bath	3 min
- 100% ethanol bath	3 min
- Xylene bath	3 min
- Xylene bath	3 min
- Xylene bath	3 min

Mount with coverslip

A.2: Atomic Force Microscope Tip-Making Protocol for Murine Tissue Indentation (Slow Drying – Colloid Method)

Tip Making Protocol (Using Slow-Drying Glue)

- Open AFM cover, turn on display (via button on AFM), and initialize software.
- Select contact mode in air experiment, and initialize stage.
- Place tip in air holder (for TMJ indentation, use center tip of HQ : NSC36, nominal K of 2)
- Place tip holder onto AFM head (CAREFULLY)
- Make sure in setup mode, place air mirror under laser.
- Note: Head will be focused close to sample, so focus on sample image, and click red crosshair onto tip that you will be using.
- Move down past sample image (laser will not be clear), and keep moving down until in reflection (laser will be more clear).
- Get sum so stage can be moved while in tip reflection.
- Move focus back up to sample, and take notice of height sensor
- Move head up 1000 micrometers (ex -3000 → -2000).
- Remove mirror.
- Place about 10 microliter of glue onto edge cover slip, place directly onto stage, and hold still with magnet.
- Move stage so edge of cover slip with glue is close to where tip is.
- In tip reflection, focus on glue, and find good location (by moving down)
- Ensure that only tip is going to impact glue (otherwise can effect future study) by making sure only tip where colloidal will attach is going into glue.
- Click on sample, refocus on glue to make sure that tip is going in right spot, and move down while in slowest movement setting (green).
- Wait 10 seconds, and then move focus up (slowest setting), then more quickly.
- MAKE SURE THERE IS AMPLE ROOM FOR COLLOIDAL PLATE
- Move 10-micrometer colloidal plate under tip, and move down focus until about 2 mm away from impact.
- Click on tip reflection, focus on colloidal (zoom in), make sure it is single colloidal.
- Click on sample view, focus by moving down, and find single colloidal again.
- Make sure it is centered under tip of cantilever, and move down in slow setting (green) until it is not possible to move anymore.
- Wait 60 seconds, and then move up in slow setting (green)
- Click back on tip reflection view, and MOVE UP to look for colloidal.
- If you can't find colloidal, it is attached to tip you are done.
- If colloidal is still there, repeat glue steps above and try to reattach another colloidal.
- Move up head, remove tip from holder (CAREFULLY MR. SHAKY HANDS)
- Do not use tip for 48 hours to allow glue to dry completely.
- Re-initialize stage, and clean up (or repeat for more tips).
- Make sure to mark what tip is what.

A.3: Atomic Force Microscope Setup, Indentation, and Data Recording Protocol for Murine Tissue Modulus Measurement

Murine Cartilage and TMJ (Condyle and Disk) Indentation Protocol

- Open AFM cover, turn on display (via button on AFM), and initialize software.
- Select contact mode in fluid experiment, and initialize stage.
- Ensure window of fluid holder is clear, if not rinse with DH2O and wipe with kimwipe.
- Place tip in fluid holder (for TMJ indentation, use center tip of HQ : NSC36, nominal K of 2)
- Make sure in setup mode, place fluid mirror under laser.
- Note: Head will be focused close to sample, so focus on sample image, and click red crosshair onto tip that you will be using.
- Move down past sample image (laser will not be clear), and keep moving head down until in reflection (laser will be more clear).
- Get as large a sum as possible (top knobs move laser)
- Zero out horizontal and vertical deflection error (side knobs)
- Remove fluid mirror.
- Using tape, remove top layer of mica from mica sample (for calibration).
- Click on navigate page on software (was on setup before)
- Place mica sample on stage, and move stage so mica is aligned under laser.
- Move AFM head down until cantilever is about 1 mm from mica.
- Use software to focus on sample (while in reflection view), and then click on sample view and repeat, until just above focus.
- Click on check parameters, and set as follows for calibration. (Scan size is 50 nm, and deflection set-point is 1 V)
- Click engage, and wait for contact.
- Once in contact with mica, click on ramp, and set parameters. Ramp size is 1 micrometer, with forward and reverse velocity also at 1 micrometer. Switch to metric, and then change trigger threshold to 3 V).
- Next, ensure graphs are correct. Channel 1 is deflection error versus z, Channel 2 is height versus z, and Channel 3 is deflection error versus time.
- Click single poke, and drag sides of top graph to linear area on right (slope is up). Click on calculate, and use this to find deflection error in air. (Only once).
- Click on spring, and enter nominal spring constant into field, and find K (in air). Bring sides in to highest peak, and fit data. From here, find spring constant. Take picture each time, and do 3 times and find average.
- Enter average calculated spring constant into proper field (possibly channel 1)
- Withdraw tip, and, and move head enough to turn mica sample.
- Cover mica layer with PBS, and add 30 microliter to just behind tip. Bring down head until meniscus forms.
- Recalibrate laser by zeroing out horizontal and vertical deflection, check for maximum amplitude.
- Check parameters (if same, good to go, if not, change to settings as in air).
- Engage, and click on ramp.

- Perform single poke, and check to ensure that there is good contact point.
- Use data as above to calculate deflection error in fluid, and save image of calculated value. Repeat two times, and average values. Enter average value into deflection error field in channel 1.
- Bring piezo head up until mica fluid meniscus breaks, and turn stage

---

- Place sample onto stage, add PBS in 30 microliter increments until sample is completely covered, and then add 30 microliter to just behind head.
- Bring head down until meniscus re-forms, and zero out horizontal and vertical deflection (check after each sample).
- Click on navigation, ensure that you are in reflection image, and then focus down on sample.
- Once focused, click on sample, and focus just above location. Dark shape, be very careful with first time location.
- Enter 1V for deflection set point (check parameters), and if having issue with 1V with disk, change to 0.5V.
- Hit engage, and click on ramp.
- Change forward/reverse velocity to 10 micrometer/s, and ramp size to 3-4 (figure out best value based on curve).
- Perform single poke. If clear impact point and good curve, capture in new folder. Repeat two more times for same location.
- Click withdraw, move slightly away from previous location (one click on slowest setting), and re-engage.
- Repeat process until 3 samples at 10 locations (can remove 2-3 if poor locations).
- Once done, withdraw, and move up piezo head until meniscus breaks. Repeat process from line until done all samples.

A.4: Cartilage Isolation and RNA Extraction Protocol Packet for Murine Knee Joint Cartilage Extraction

(Last Updated: 11/29/15)
Han Laboratory Group

Dissection of Mouse Knee (Updated 11/16/15)

- Make incision at base of mouse pelvis, to remove fur.
- Pull fur down past knee joint, as far as possible.
- Cut through hip joint, and at ankle of mouse to ensure adequate long bone to work with while performing further dissection.
- Trim away secondary structures, patellar tendon, synovial capsule, taking care not to damage meniscus.


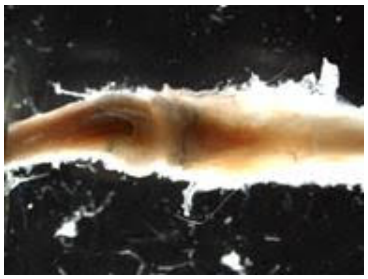


- Sever MCL and LCL to loosen joint (you can play with knee bending to see what ligaments are left to be cut)
- If you want to save meniscus, be careful when cutting PCL and ACL.
- Bend joint completely, and look for ACL, and then cut it, being careful not to damage meniscus with small scissors.
- Continue cutting soft tissues around joint, until you can completely sever tibia from femur.
- Place femur and tibia into HBSS or PBS solution to ensure tissue does not dehydrate
- Trim as much tissue from around femur and tibia as possible, while taking care not to damage cartilage.
- Place samples back into HBSS or PBS until ready to trim cartilage. (Note: it should look like this:)

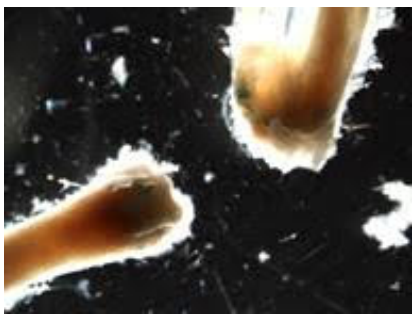


Cartilage and Chondrocyte Isolation (Updated 11/29/15)

- Trim cartilage from both femur and tibia at epiphyses; consult the image below.

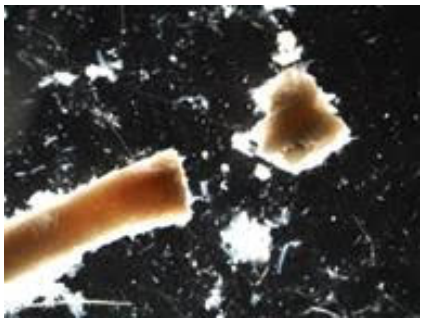
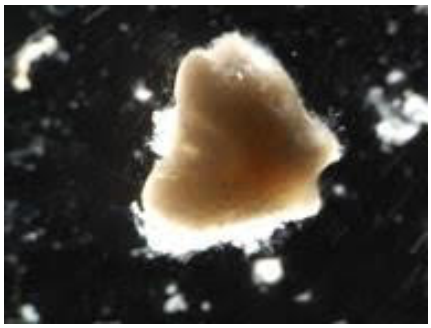

- Place 4-5 femurs/tibias in collagenase solution tubes (instructions for creation in appendix)
- Vortex each tube for approximately 5 seconds.
- Place in 37 °C incubator or water bath for 2-3 hours (depending on size of cartilage sample, larger = longer)
- Remove any large particles with thin tweezers, and then spin tubes down at 2,000 RPM in centrifuge for 15 minutes.
- There should be whitish cell pellet at bottom of tube.
- Remove supernatant, and add fresh HBSS and re-immerse the cells back into solution.
- Perform next step as soon as possible.

Chondrocyte Cell Purification (Updated 11/29/15)

- Filter for cells only with 70 micrometer pore size filter, use with 50 mL conical tubes, diluting with PBS/HBSS to ensure cells pass through filter
- Count cells to ensure viable sample (want at least 100,000 cells per sample in order to have enough RNA to perform RT-PCR).
- Spin down cells at 1,000-1,500 RPM for 5-10 minutes to create cell pellet, and then remove supernatant.
- Add 1 mL of buffer solution, mix, and then transfer to smaller 1-2 mL conical tube.
- Spin down again to create cell pellet, and then remove supernatant.
- Add TRIzol reagent (500 microliter) to each cell pellet, and then mix.
- Store at -80°C (can be stored for several months if needed).

RNA Isolation (Updated 11/29/15)

Note: This method adapted from Wei Tong at Penn Lab

- Let TRI-zol/cell solution thaw at room temperature until liquid
- Add 50 µL of 1-bromo-3-chloropropane to solution (1/10 of initial solution volume)

- Vortex vigorously for 30 seconds, then centrifuge (12,000 g) at 4°C for 15 minutes (ensure cap is facing outward from centrifuge to make it easier to extract RNA.
- Three layers should form, collect top phase carefully. (Better to get less than contaminate with middle phase.)
- Add 250 µL 2-propanol (1/2 volume TRI-zol), then vortex 30 seconds.
- Let stand for 10 min at room temp, then centrifuge 12,000g for 10 min at 4 °C.
- Remove supernatant, and add 500 µL of 75% ethanol (specific for PCR use) (should be same amount as added TRIzol)
- Vortex briefly, and then spin at 7500 g for 5 minutes at 4° C.
- Remove as much ethanol as possible carefully to speed up drying time.
- Check every 3 minutes, as soon as ethanol completely disappears, add RNA-free water (10-50 µL).
- Store at -80° C until ready to proceed with experiment.